

**Correlations and Preliminary Validation of Laboratory Asphalt
Binder and HMA Reflective Cracking Resistance to Field
Performance of In-Service Highway Sections**

By

Oswaldo De Jesús Guerrero Bustamante

Civil Engineer

Master's Thesis in Civil Engineering

Luis Fuentes, Ph.D.

Lubinda F. Walubita, Ph.D.

Thesis Advisors



Department of Civil and Environmental Engineering

Universidad del Norte

Barranquilla, Colombia

November 2019

ABSTRACT

Reflective cracking is one of the dominant distress modes occurring when hot-mix asphalt (HMA) overlays are placed over existing cracked flexible and/or jointed rigid pavements. Various tests have been conducted in the literature for measuring, characterizing, and quantifying the cracking resistance potential of HMA mixes in the laboratory. Asphalt-binder is one of the key constituent elements that significantly influences and controls the fracture behavior and cracking performance of hot-mix asphalt (HMA), both in the laboratory and field. In particular, the low-temperature rheological properties of the asphalt-binders are very critical in terms of improving the HMA fracture properties in the laboratory and ultimately mitigating cracking in the field. The Elastic Recovery (*ER*) and Bending Beam Rheometer (*BBR*) are the most widely used laboratory test methods for evaluating and quantifying the asphalt-binder behavior at low temperatures, mostly using the *ductility* (*ER*), *stiffness* (*S*), and *m-value* parameters. Some cracking test related to mixes have been studied, both of dynamic and monotonic loading modes. However, one key challenge with most of these laboratory tests is correlations and validation with field performance data. Quite often, field data availability is a challenge or otherwise, needs costly long-term performance monitoring.

Using the Texas flexible pavements and overlays database, namely the Texas Data Storage System (DSS), as the data source, this study was conducted to correlate and preliminarily validate the asphalt-binder low-temperature properties (measured using the BBR and ER tests) and laboratory monotonic-loading overlay tester (OT) to the field crack (reflective) performance of in-service highway sections.

In general, while the asphalt-binder low temperature properties (*ER*, *m-value*, and *S*) exhibited promising potential to predict the HMA fracture properties from the M-OT test, namely *tensile strain* (ϵ_t) and *Fracture Energy Index* (*FE Index*), with a coefficient of determination (R^2) greater than 60%, this was not the case with the field cracking performance data. Statistical correlations, with over 60% accuracy/certainty (i.e., $R^2 > 60\%$) were obtained only for the case where the field cracking performance data was analyzed and normalized to an equivalent number of traffic loading ESALs. The rest of the parameters indicated predictive accuracy/certainty lower than 50%. Overall, these findings may suggest that the asphalt-binder low temperature properties from the ER and BBR tests must be interpreted and applied cautiously when directly relating to and/or predicting the field cracking performance of the corresponding HMA mixes.

However, the monotonic-loading OT test exhibited promising potential as a repeatable test (coefficient of variation [COV] < 30%) for evaluating and quantifying the cracking resistance potential of HMA mixes in the laboratory relative to the field performance of in-service highway sections. In particular, the following HMA fracture parameters, fracture energy (*FE*), tensile strength (σ_t), *FE Index*, and peak load (P_{max}) from the monotonic-loading OT test, with COV values less than 30%, were able to statistically differentiate the HMA mixes (statistical groups ≥ 2) and also correlated well (coefficient of determination [R^2] > 60%) with the measured field cracking performance data.

*I dedicate this thesis to my parents, Oswaldo and
Milagros, to my siblings, Nicolas and Maria, whom I love
more than anything in the world.*

ACKNOWLEDGMENTS

I would like to express my deep and sincere gratitude to Dr. Luis Fuentes and Dr. Lubinda F. Walubita for their continuous support, assistance, time, patience, motivation and constructive advice during the research work. Your guidance and supervising are appreciated and helped me to achieve this important goal.

A special thanks to my parents, my siblings for always giving me their support and love during these years, without them it would not have been possible. Thank you for believing in me and motivating me to do great things.

Lastly, but not the least, I would like to thank all the agencies/institutions that provided financial and technical support towards the development of the Texas flexible pavements and overlays database (the Texas DSS) project, which valuably served as the data source for the research work presented herein. In particular, much appreciation and gratitude go to all the individuals who worked on the Texas DSS.

TABLE OF CONTENTS

LIST OF FIGURES	VII
LIST OF TABLES	VIII
CHAPTER 1.....	9
INTRODUCTION.....	9
1.1. Problem Statement.....	9
1.2. Research Objectives	11
1.3. Articles Derived from the Study	12
1.4. Structure of the Thesis	12
1.5. Summary	13
CHAPTER 2.....	15
LITERATURE REVIEW	15
2.1. Reflective Cracking Phenomenon	15
2.2. Asphalt Binder Cracking Evaluation.....	16
2.3. HMA Cracking Evaluation	17
2.4. Summary	19
CHAPTER 3.....	20
EXPERIMENTAL DESIGN PLAN.....	20
3.1. Texas Data Storage System (DSS).....	21
3.2. Materials and HMA Mix-Designs	21
3.3. Highway Test Sections and Field Characteristics	22
3.4. Pavement Structures and Existing Distress Conditions.....	23
3.5. Summary	24
CHAPTER 4.....	25
LABORATORY TEST RESULTS AND ANALYSIS.....	25
4.1. Asphalt Binder Laboratory Test Results.....	25
4.1.1. Elastic Recovery (<i>ER</i>).....	25
4.1.2. Bending Beam Rheometer (<i>BBR</i>).....	26
4.2. Hot Mix Asphalt Laboratory Test Results.....	29
4.2.1. Statistical Analysis (ANOVA and Tukey's HSD).....	32
4.3. Laboratory Test Comparisons and Rankings	35
4.4. Test Repeatability and Data Quality.....	36
4.5. Synthesis and Discussion	37
4.6. Summary	38
CHAPTER 5.....	39
FIELD PERFORMANCE RESULTS AND ANALYSIS	39

CHAPTER 6.....	47
LABORATORY AND FIELD CORRELATIONS.....	47
6.1. Correlations of Asphalt Binder Laboratory Test Results.....	47
6.2. Correlations of Laboratory Asphalt Binder to HMA Fracture Properties	48
6.2.1. Asphalt-Binder Elastic Recovery (ER) versus HMA Fracture (M-OT) Properties.	49
6.2.2. Asphalt-Binder Bending Beam Rheometer (BBR) versus HMA Fracture (M-OT) Properties.	50
6.3. Correlations of Laboratory Asphalt Binder to Field Performance	53
6.3.1. Asphalt-Binder Elastic Recovery (ER) versus Field Cracking Performance.....	53
6.3.2. Asphalt-Binder Bending Beam Rheometer (BBR) versus Field Cracking Performance	54
6.4. Fracture (M-OT) Properties versus Field Performance	57
6.5. Summary	61
CHAPTER 7.....	63
SUMMARY, CONCLUSIONS AND RECOMMENDATIONS	63
7.1. Synthesis and Discussion of the Results and Findings.....	63
7.2. Conclusions	64
7.3. Significance and Application of the Study Results and Findings	67
7.4. Limitations and Challenges of the Study.....	67
7.5. Recommendations for Future Research.....	68
REFERENCES	69
APPENDICES.....	75
A. Database.....	75
B. R Codes Results	75

LIST OF FIGURES

Figure 1. Induction and Mechanisms of Reflective Cracking.....	9
Figure 2. Study Work Plan and Thesis Structure.	14
Figure 3. Stresses and crack growth in an overlay due to traffic [14], [39].....	15
Figure 4 Schematic Illustration of the Experimental Design Plan.	20
Figure 5 Elastic recovery test: (a) asphalt-binder specimen; (b) sample after 20 cm elongation; (c) sample cut in the midpoint and resting.	25
Figure 6. BBR definition of the m-value.....	27
Figure 7. Monotonic-Loading OT Test Setup.	29
Figure 8 Monotonic-Loading loading OT L-D Response Curve [30].	30
Figure 9 HMA Fracture Parameter's average COV	37
Figure 10. Pavement Surface Condition (Spring 2019).	40
Figure 11. Reflective Cracking Performance versus Time.	42
Figure 12. Reflective Cracking Performance versus Traffic Loading.	44
Figure 13. Asphalt-Binder Low Temperature Correlations.	48
Figure 14. Asphalt-Binder Elastic Recovery - Tensile Modulus and Tensile Strain Correlation.	49
Figure 15. Asphalt-Binder Elastic Recovery – Peak Load and Tensile Strength Correlation.	49
Figure 16. Asphalt-Binder Elastic Recovery – FE and FEI Correlation.....	50
Figure 17. Asphalt-Binder HMA Correlations.	51
Figure 18. ER – Approach D Correlation.	54
Figure 19. ER – Approach F Correlation.	54
Figure 20. BBR-Field Reflective Cracking Correlation Plots.....	56
Figure 21. Relationship between Monotonic OT parameters and field performance in the (a) Reflection cracking as a function of time (b) Rate of reflective cracking per year (c) Reflection cracking as a function of traffic loading (d) Initiation phase (e) Initiation and propagation phase (f) Propagation phase	60

LIST OF TABLES

Table 1 Asphalt-Binders and HMA Mix-Design Characteristics.....	21
Table 2 Highway (Overlays) Test Sections.....	22
Table 3. Highway Pavement Structures.....	23
Table 4. Data Analysis Models for ER.....	25
Table 5. Asphalt-Binder ER Test Results.....	26
Table 6. Data Analysis Models for BBR.....	27
Table 7. Asphalt-Binder BBR Test Results.....	28
Table 8. Data Analysis Models for M-OT.....	30
Table 9. Monotonic Overlay Test Results.....	31
Table 10. Statistical Analysis ANOVA y Tukey's HSD for Peak Load.....	33
Table 11. Statistical Analysis ANOVA y Tukey's HSD for Tensile Strength.....	33
Table 12. Statistical Analysis ANOVA y Tukey's HSD for Tensile Strain.....	34
Table 13. Statistical Analysis ANOVA y Tukey's HSD for Tensile Modulus.....	34
Table 14. Statistical Analysis ANOVA y Tukey's HSD for Fracture Energy.....	34
Table 15. Statistical Analysis ANOVA y Tukey's HSD for Fracture Energy Index.....	34
Table 16. ANOVA and Tukey's HSD Test Analyses.....	35
Table 17. Laboratory HMA and Asphalt-Binder Ranking.....	36
Table 18. Rate of Reflective Cracking per Traffic Loading ESAL (%Cracking/MESAL). 45	
Table 19. HMA Mix Field Performance Ranking.....	46
Table 20. Field Cracking Performance Parameters.....	47
Table 21. Regression Coefficients α , β , and R^2 for Asphalt Binder to HMA Fracture Properties.....	52
Table 22. Regression Coefficients m , b and R^2 in Equation 11.....	56
Table 23. Regression Coefficients α , β and R^2 in Equation 12.....	60

CHAPTER 1 INTRODUCTION

1.1. Problem Statement

Around the world hot mix-asphalt (HMA) overlays is one of the most common alternatives used for rehabilitating deteriorated flexible and rigid pavements. This resurfacing technique is a quick and cost-effective solution for the governmental institutions that re-establishes the surface smoothness, restores the skid resistance, strengthens the bearing capacity of the existing pavement [1]. However, when an HMA overlay is placed over an existing cracked or jointed pavement, these cracks or joints will undesirably reflect on the overlaid pavement surface in a relative short period of time, namely as reflective cracking. Therefore, the life of an HMA overlay is strongly influenced by this type of distress. Reflective cracking is primarily caused by the repetitive tensile stresses due to temperature variations and/or traffic loading that generate horizontal and vertical movements in the pavement structure [2]–[4]. The rate of crack propagation is dependent on the condition of the existing pavement and the thickness of the overlay, among other factors [2]. Figure 1 exemplifies the effects of temperature (thermal induced), traffic loading, and surface contraction (thermal) on the induction of reflective cracking [5], [6].

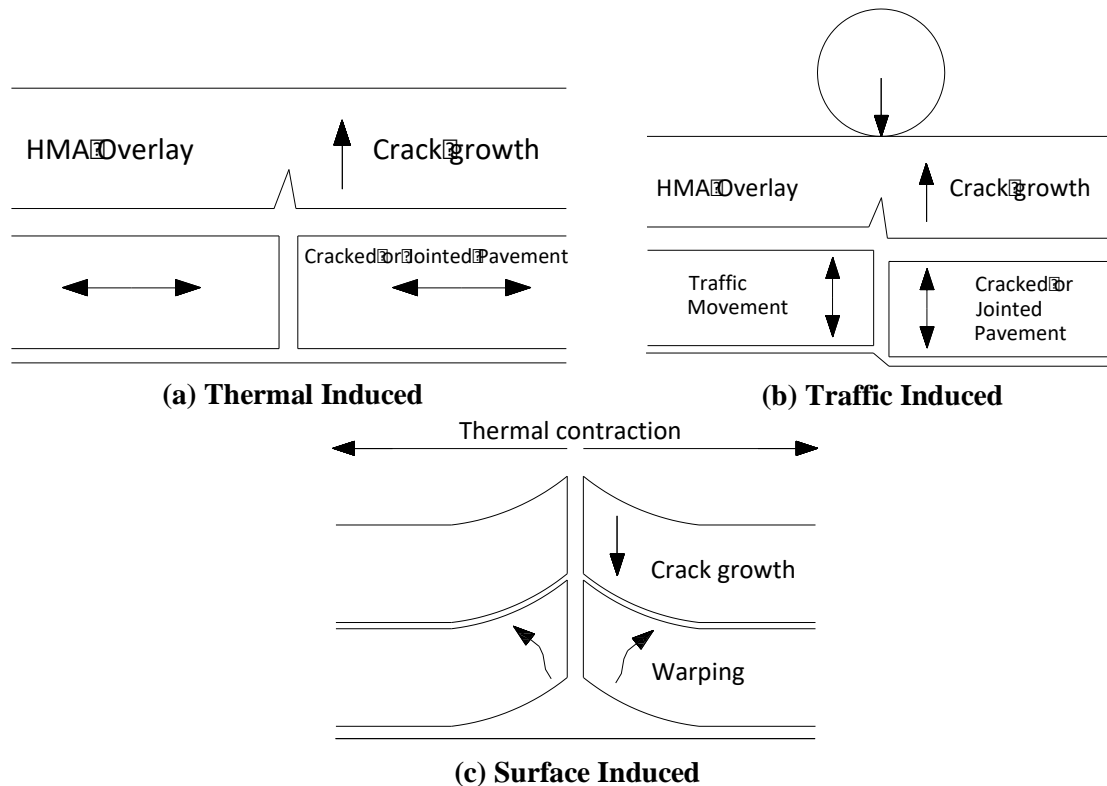


Figure 1. Induction and Mechanisms of Reflective Cracking.

One of the key challenges of resurfacing deteriorated flexible and rigid pavements is to control the reflective cracking phenomenon. Despite all the efforts that researchers

continuously make in order to develop and improve existing technologies in the pavement engineering field, this type of distress is still a prevalent issue of concern – costing highway agencies millions of dollars in maintenance and rehabilitation activities [7]–[12]. Furthermore, cracking can also induce other distresses, cause structural damage, and/or accelerate the rate of pavement deterioration. Water infiltration through the cracks, for instance, can undesirably lead to moisture damage in the underlying pavement layers. Similarly, excessive air ingress through the cracks can lead to rapid oxidative aging of the asphalt-binder (in the case of HMA pavements) – ultimately, affecting the long-term performance and durability of the entire pavement structure [12]. In 2003, Zhou et al. [13] reported that cracking had a detrimental effect on pavement surface roughness and needed to be timely mitigated.

Numerous studies have been conducted in order to reduce or prevent the reflective cracking phenomenon in asphalt pavement, evaluating the variables that influence this distress such as the thickness of the overlay [6], the use of geotextiles or interlayer membranes [14], [15], special treatments to the underlying layers such as crushing, fracturing or rubblization [7], [16]. Dhakal et al. [5] conducted a study to evaluate the most common treatments methods to control the reflection cracking, with estimated costs that vary between 1 – 10 USD/yd². Cleveland et al [8] categorized four methods that are commonly employed in the field to reduce or control reflective cracking:

- a) increase the HMA overlay thickness
- b) perform special treatments on the existing surface
- c) special treatments on the cracks and/or joints
- d) special considerations of the HMA overlay design

One of the options for mitigating cracking in HMA is to improve the rheological properties of the asphalt-binders. Hu et al [17] conducted a study to demonstrate the influence of asphalt-binder source on the rutting and cracking performance of HMA. The Superpave asphalt-binder specification has proposed some rheological parameters to evaluate and quantify the contribution of asphalt-binder in the performance of HMA mixes [18]. There are some laboratory tests proposed in the literature to measure, characterize, and quantify the cracking resistance potential of HMA mixes relating to asphalt binder [18]–[21]. However, these tests are considered empirical without detailed fundamental analysis, do not adequately represent the fracture behavior of the asphalt-binder and HMA under real field conditions, and without validation with field performance data [22]–[25].

As mentioned before, the focus of this study is reflective cracking. Various studies has been conducted to develop and improve the laboratory testing procedures for effective evaluation, quantification and prediction of the reflective cracking resistance potential of HMA mixes [2], [9], [15]. Currently, one can find different test methodologies and criteria that aim to screen and produced crack-resistant HMA mixes during the mix-design stage in the laboratory [26]–[30].

The commonly used laboratory test methods for measuring the asphalt-binder properties related to HMA cracking at low temperatures (≤ 10 °C) include the Bending Beam Rheometer (BBR) and Elastic Recovery (ER) [17], [31]. Other available laboratory test

methods include the penetration and, softening point tests, – but these tests are considered empirical without detailed fundamental analysis to represent the fracture behavior. With the introduction of the Superpave performance-grading (PG) system, researchers have focused their attention on identifying the critical rheological properties that are directly related to the field performance of asphalt-binders and HMA [25]. To effectively predict the contribution of asphalt-binders to the performance of the HMA in the pavement structures, the Superpave PG system includes measuring performance-related rheological properties (of the asphalt-binders) under laboratory conditions that simulate field conditions, namely climate and traffic loading [32].

Similarly, the need of reliable performance tests to effectively predict the fracture behavior of HMA mixes has led researchers to develop different HMA cracking tests, for both dynamic and monotonic loading modes [9], [33]. One of such laboratory tests is the monotonic-loading Overlay Tester (M-OT) [9], [33].

In this study, only HMA monotonic loading test were evaluated, because these generally tend to be simpler and have low variability in their responses (i.e., coefficient of variation, COV $\leq 30\%$) than the repeated or dynamic-loading tests [33], [34]. In addition to have lower variability, most monotonic loading tests are also easier to set up, cheaper and require a shorter test time than dynamic load tests. In addition to being repeatable, most monotonic-loading crack tests are also practically easier/simpler to set up and more cost-effective, i.e., shorter test time. However, most of the monotonic-loading crack tests, including the monotonic-loading OT test that is the subject of this study, have no proven historical records of satisfactorily correlating to field cracking performance [11], [12], [30], [33], [35]–[38]. Which involves that one key challenge with most of these laboratory tests is how to correlate and validate them with field performance data. Quite often, field data availability is a challenge or otherwise, needs costly long-term performance monitoring. Thus, having a long-term database (although costly), as will be discussed and presented subsequently in this document, is vital to help with correlating and validating some of these laboratory tests with field cracking performance data.

As presented and discussed subsequently, two laboratory asphalt-binder tests (namely the Bending Beam Rheometer and Elastic Recovery), and the monotonic loading overlay test (as well as the monotonic-loading OT), in relation to field HMA cracking performance of in-service highway (overlay) sections, are the subject of this study.

1.2. Research Objectives

Based on the foregoing background, the primary goal of this study was to correlate and preliminarily validate the laboratory asphalt binder low temperature properties and monotonic-loading OT test to field crack performance of in-service highway sections. Considering the limitations of previous studies as well as the fact that there is no conclusive evidence on the direct correlation between most of the existing laboratory test methods and field cracking performance data, the specific objectives of the study were devised as follows:

- a) Determine and quantify the asphalt-binder low temperature properties (using the BBR and ER) of different Texas asphalt-binders from the Texas flexible pavements and overlays database (DSS).
- b) Determine and quantify the HMA fracture properties of different Texas mixes using the monotonic-loading OT test data from the Texas flexible pavements and overlays database (DSS).
- c) Comparatively rank the mixes in terms of their laboratory cracking resistance potential for each asphalt binder low temperature properties and HMA fracture parameter.
- d) Comparatively assess which of the HMA fracture parameter (s) has the least statistical variability and associated with more statistical reliability.
- e) Assess the ability of each of the fracture parameters obtained from the monotonic loading Overlay Test to statistically differentiate between asphalt concrete mixtures.
- f) Evaluate and comparatively rank the field cracking performance of the HMA mixes on various in-service highway sections from the DSS.
- g) Correlate the asphalt-binder low temperature properties (*elastic recovery*, *m-value*, and *S*) to the monotonic loading OT HMA fracture parameters.
- h) Correlate the laboratory test data to field HMA reflective cracking performance and establish which asphalt-binder parameter(s) provides the best statistical correlation.
- i) Correlate the laboratory test data to field cracking performance and establish which HMA fracture parameter(s) provides the best statistical correlation.

1.3. Articles Derived from the Study

From this thesis, the following papers were developed:

- Walubita, L., Fuentes, L., Lee, S.I., Guerrero, O., Mahmoud, E., Naik, B. (2019), Correlations and Preliminary Validation of the Laboratory Monotonic Overlay Test (OT) Data to Reflective Cracking Performance of In-service Field Highway Sections. Submitted to Journal of Construction and Building Materials.
- Walubita, L., Guerrero, O., Mahmoud, E., Fuentes, L., Lee, S.I., Zhang, J. (2019), Correlating the Asphalt-Binder Low Temperature Properties to HMA Field Cracking Performance of In-service Field Highway Sections. Submitted to Journal of Construction and Building Materials.

1.4. Structure of the Thesis

To achieve the objectives of the study, the structure of the thesis, in addition to this introduction (Chapter 1), has been organized as follows:

- Chapter 2 provides an overview of the relevant literature associated with the fundamental concepts of the reflective cracking phenomenon, the asphalt binder and the HMA cracking evaluation.
- Chapter 3 describes the experimental design plan, including the asphalt concrete mixes used, the road test sections in service and their pavement structures.

- Chapter 4 presents and analyze the laboratory test results, including the measured asphalt binder low temperature and HMA fracture properties obtained from the BBR, ER and M-OT.
- Chapter 5 presents the field performance data of the six selected sections obtained from the Texas Flexible Pavements and Overlays Database (DSS).
- Chapter 6 presents the laboratory predictions and the field correlations analysis conducted with the laboratory test results and the field performance data.
- Chapter 7 synthesizes, discuss and conclude the results and key findings, the significance and the limitations of the study. Finally, some recommendations are given for future work.

Figure 2, on the next page, illustrates the organizational flow chart for the study work plan and structure of the thesis.

1.5. Summary

This introductory chapter discussed the background, problem statement and study objectives. Some article publications derived from the study were then presented, followed by the structure of the thesis and the work plan. Some appendices containing important data are also included at the end of the thesis.

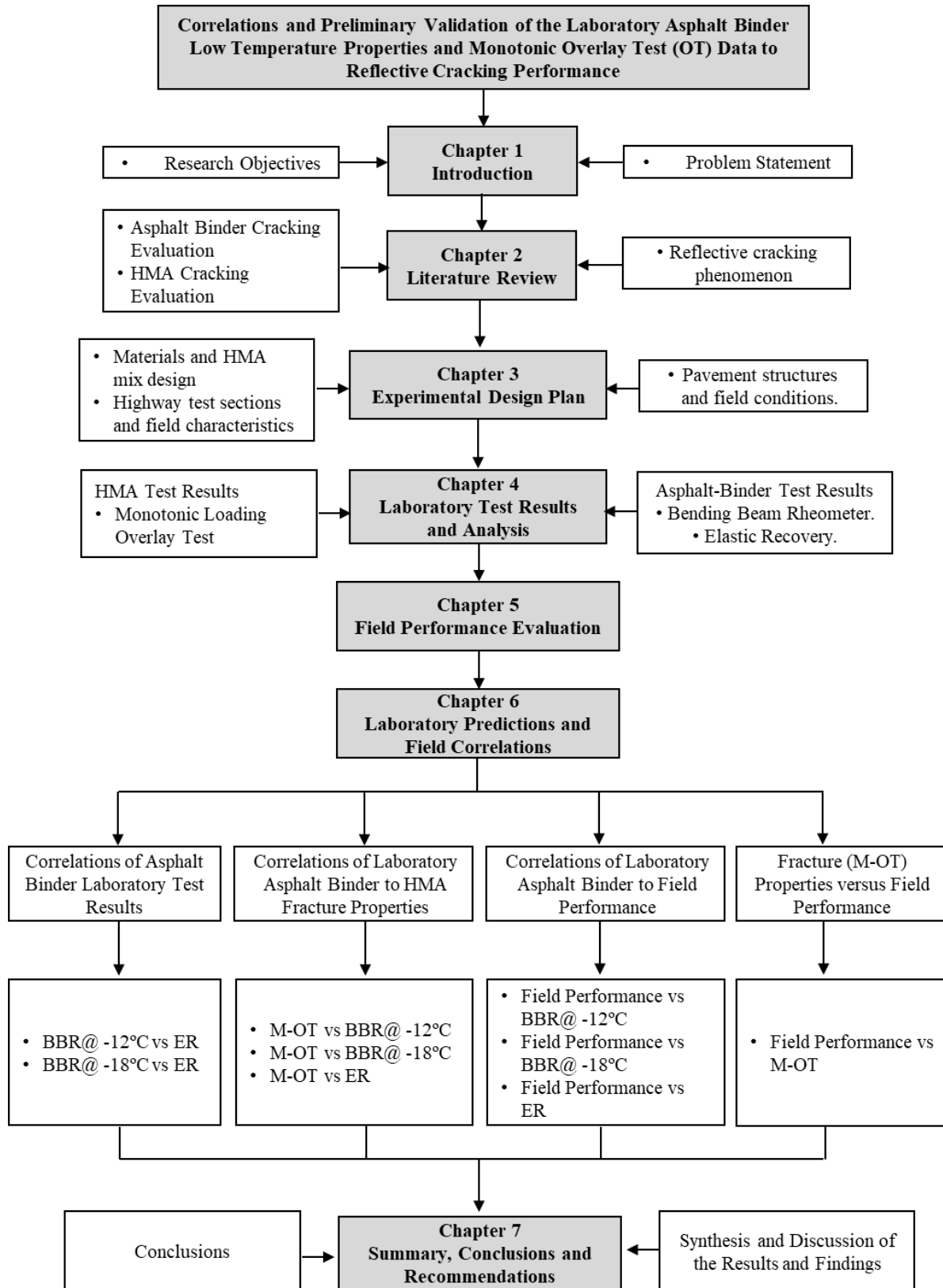


Figure 2. Study Work Plan and Thesis Structure.

CHAPTER 2 LITERATURE REVIEW

2.1. Reflective Cracking Phenomenon

The fundamental principle of the reflective cracking phenomenon is that the tensile stresses at the interface of the crack or joint and the new HMA overlay are significantly increased due to the discontinuity, this stresses rapidly exceed the tensile strength of the HMA overlay and the crack initiates at the interface and quickly propagates to the surface [2]. Reflection cracks is produced by a joint effect of traffic loads and temperature changes that generate vertical and horizontal movements in the pavement structure [3], [4]. Lytton (1989) [14] said that a every pass of a traffic load over a crack or joint would induce three maximum pulses, two peak shearing stresses and one bending peak stress in the HMA overlay as can be seen in Figure 3. The first stress pulse is a maximum shear stress pulse presented at Point A in Figure 3, this stress is produced by the movement or displacement induced by the load of traffic on a plate or portion of it with respect to the next. The second stress pulse is a maximum bending stress pulse shown at Point B in Figure 3. The third stress pulse is again a maximum shear stress pulse in the Point C, except that it is in the opposite direction to the previous shear stress pulse [14].

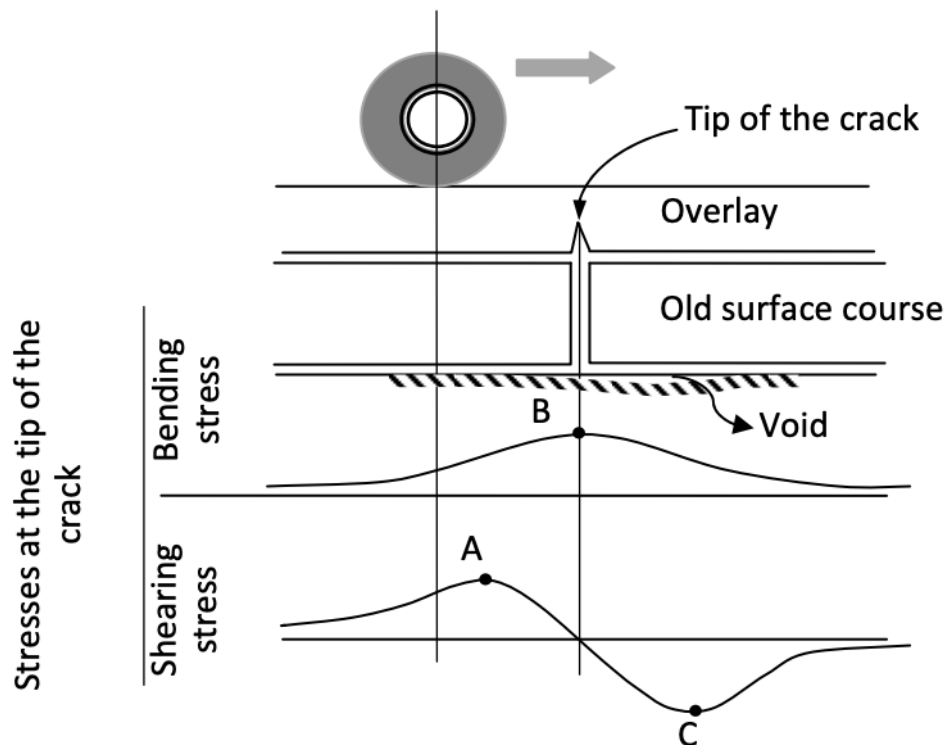


Figure 3. Stresses and crack growth in an overlay due to traffic [14], [39].

In general, a cracked pavement structure can be loaded in any one or a combination of the three fracture modes [40]: (i) Mode I or opening mode, results from loads that are applied

normally to the crack plane (thermal and traffic loading). (ii) Mode II or sliding mode results from in-plane shear loading, which leads to crack faces sliding against each other normal to the leading edge of the crack (traffic loading). (iii) Mode III or tearing mode, results from out-of-plane shear loading, which causes sliding of the crack faces parallel to the crack leading edge. This mode of loading is considered negligible for pavements. A schematic of the three fracture modes is illustrated in Figure 1.

In general, the research efforts to avoid reflection cracking has historically had two main approaches: a) reduce the magnitude of the tensile stresses at the crack-overlay interface (e.g. rubblization) or b) increase the tensile strength of the HMA overlay (e.g. increasing the overlay thickness, geotextiles) [2]. As mentioned before, numerous studies have been conducted in order to reduce or prevent the reflective cracking phenomenon in asphalt overlay pavement, evaluating the variables that influence this distress such as the thickness of the overlay [6], the use of geotextiles or interlayer membranes [14], [15], special treatments to the underlying layers such as crushing, fracturing or rubblization [7], [16].

2.2. Asphalt Binder Cracking Evaluation

Most of the methodologies for evaluating the asphalt-binder response to cracking performance are based on the original Superpave PG specification for cracking and fracture, using the complex shear modulus viscous portion ($G^* \sin \delta$) parameter [19], [32]. This parameter is based on evaluating the amount of energy that the asphalt-binder can dissipate over the course of one load cycle [32]. However, some authors have reported that there is a poor correlation between the Superpave criterion $G^* \sin \delta$ and the HMA cracking performance [41], [42]. In particular, this parameter appears not to be sufficient for characterizing the properties of polymer-modified asphalt-binders relative to HMA fatigue performance [43]. Bahia et al. [44] suggested that cracking damage should not be predicted using only linear viscoelastic properties. Some laboratory test methods such as the dynamic shear rheometer (DSR), using the time sweep concept, have also been proposed as an alternative test method for fatigue evaluation of asphalt-binders [45].

The Superpave PG methodology was developed between 1987 and 1993 during the Asphalt Research Program of the Strategic Highway Research Program (SHRP) as a fundamental means to accurately characterize and quantify the rheological properties of asphalt-binders for use in HMA pavements [18]. The Superpave PG system essentially established a methodology that included a more detailed and complex analysis of the deterioration phenomenon of HMA in the temperature ranges that the asphalt-binder is actually exposed to during its service life. The PG methodological approach was conceptualized on the idea that the measured properties of the asphalt-binder should simulate and be directly related to field conditions [23]. The Superpave PG system classifies the asphalt-binders taking into account the upper and lower working-service temperatures, which the asphalt-binders are subjected to in the field [46].

The PG system established by Superpave suggest that asphalt-binder samples must be tested in the temperature ranges that the asphalt-binder will be exposed to during its service life. This is conceptualized on the idea that the properties of an asphalt-binder should be related to field conditions [23]. This implies that the cracking performance of asphalt-binders and

HMA mixes should be measured at low temperature. The BBR test has been recommended, based on the Superpave PG system, to measure and characterize the low-temperature properties of the asphalt-binders [19]. The low temperature asphalt-binder specification is defined by the AASHTO M320 and ASTM D6373 [47], [48]. Hesp et al. [49] proved that the current low temperature asphalt-binder specifications, namely AASHTO M320 and ASTM D6373, showed a 55% accuracy and a complete inability to correctly predict crack failures, suggesting the need to improve the low-temperature specification grading [47], [48]. Field data collected suggested that asphalt-binders with the same grade have a completely different performance [49]. Tabib et al [50] showed a moderate to excellent correlation for the performance grade (low-temperature) with field pavement cracking (i.e., coefficient of determination [R^2] > 80%).

The percent Elastic Recovery (*ER*) is used by many highways agencies for modified bitumen grading specifications [51], trying to evaluate/quantify the elastic properties of asphalt binder measuring the amount of recoverable deformation. The ER can be measured using two simple asphalt-binder tests: ER test (using a ductility device) and Multiple Stress Creep Recovery (*MSCR*) test using the DSR [21], [52]. Some studies have indicated that getting higher ER is a good indicator to resist cracking [53]–[57]. Zhang et al. [43] conducted a laboratory study to further analyze the relationships between the asphalt-binder ER properties and the HMA cracking resistance and fracture properties, respectively. The study indicated that HMA mixes with high ER properties showed better laboratory cracking resistance performance and superior HMA fracture properties measured with the dynamic-loading OT test [43].

The Bending Beam Rheometer (BBR), primarily based on the *stiffness* (*S*) and *m-value* parameters, is a dominant Superpave laboratory test used to measure, characterize, quantify, and grade (PG) the low-temperature properties of the asphalt-binders relative to HMA cracking [24]. The ER test, on the other hand, measures the degree to which the material recovers to its original position following an application and release of a tensile loading [58].

It is important to mention, in turn, that these approaches that seek to evaluate cracking performance of asphalt mixes from bitumen do not take into account the portion of aggregates, which constitutes about 90-95% of the total mixture by weight [59]. This methodologies has received many criticisms in the scientific community for its simplicity to explain such a complex phenomenon, and alternatives such as frequency sweep using the dynamic shear rheometer have been proposed as better options for the evaluation of asphalt to cracking response [45].

2.3. HMA Cracking Evaluation

A large number of research articles have been carried out in the last 20 years with the aim of developing and improving the asphalt mixture test procedures to evaluate and other even predict crack resistance of asphalt mixtures [3], [4], [60]. Depending on the cause, mechanism, location of occurrence, etc., different modes of HMA pavement crack failure are identifiable in the field including thermally induced, reflection, bottom-up fatigue, and top-down fatigue cracking [9]. Considering the aforementioned, different test methods have been proposed to evaluate the cracking potential of HMA in the laboratory, and it is possible to relate different laboratory test methods with a specific cracking failure mode. Table 1

summarizes the commonly used laboratory test methods grouped as a function of the HMA crack failure mode [9].

Table 1. HMA Crack Failure Modes and Commonly Used Lab Test Methods.

Thermal Cracking Test	Reflection Cracking Test	Bottom-up Fatigue Cracking Test	Top-Down Cracking Test
DSCTT	OT	Beam Fatigue	IDT-Florida
SCB	FBBF	S-VECD	SCB-LTRC
SCB-IL	SCB-LTRC	Repeated Tension	S-VECD
IDT	DSCTT	OT	Repeated Tension
TSRST/UTSST	IDT	SCB-LTRC	Modified OT

Legend: IDT = Indirect Tension
 SCB = Semi Circular Bend
 DSCTT = Disk Shape Compact Tension
 OT = Overlay Test
 IL = Illinois

TSRST = Thermal Stress-Restrained Specimen Test
 FBBF = Flexural Bending Beam Fatigue
 S-VECD = Simplified Viscoelastic Continuum Damage
 UTSST = Uniaxial Thermal Stress and Strain Test
 LTRC = Louisiana Transportation Research Center

Some of the monotonic-loading crack tests reviewed in the literature include the IDT, monotonic-loading OT, DSCTT, monotonic-loading SCB, etc. [9], [33]. These test methods have been used to measure, evaluate, characterize, screen, and sometimes predict the cracking resistance performance of HMA mixes. However, none of these test methods has been universally adopted for routine mix-design and screening for HMA crack evaluation because of their inherent pros and cons – that are discussed subsequently [35]. As discussed previously, another challenge is their predictive accuracy, validation, and correlation with field cracking performance data.

The laboratory cracking test methods can be divided into two categories depending on the loading mode, as follows: cyclic (dynamic) and monotonic [3]. This study focuses on the monotonic-loading tests that are generally simpler and more repeatable with low test-data variability (i.e., coefficient of variation [COV] $\leq 30\%$) than the dynamic-loading tests [33], [34]. In addition to being repeatable, most monotonic-loading crack tests are also practically easier/simpler to set up and more cost-effective, i.e., shorter test time. However, one key challenge with most of these laboratory tests is how to correlate and validate them with field performance data. Quite often, field data availability is a challenge or otherwise, needs costly long-term performance monitoring. Thus, having a long-term database (although costly), as will be discussed and presented subsequently in this paper, is vital to help with correlating and validating some of these laboratory tests with field cracking performance data.

In their study, Walubita et al., [35] suggested that the monotonic-loading OT and IDT tests could be used as routine tests to evaluate the crack resistance of HMA due partly to their simplicity, short running time, and cost-effectiveness in lieu of their dynamic-loading counterparts. However, validation of these tests with field data remains one of the most cited challenges [35], [37]. The difficulty associated with the sample preparation and test set up of the DSCTT limits its use for daily routine applications [30]. The SCB, on the other hand, is generally suited for low and intermediate temperature testing (crack evaluation) [34].

In terms of test repeatability, studies conducted by Walubita et al., [12], [30], [33], [35] to compare the OT, IDT, and SCB tests (solely based on Texas mixes tested at 25 °C) found that the monotonic-loading OT and IDT tests (at 25 °C) were more repeatable with lower

variability in the test data than the SCB test. However, Nsengiyumva [59] reported that the SCB test provides a practical and repeatable test methodology to characterize the HMA fracture behavior and propensity to cracking with statistically acceptable results at intermediate to low temperatures. Nsengiyumva [59] contends that the test data inconsistency reported in other publications is partly attributed to the selected test variables such as the test temperature. In general, cracking tests based on monotonic loading are fairly repeatable with acceptable statistical variability and low COV values, less than 30% [9]. However, most of these monotonic-loading crack tests, including the monotonic-loading OT test that is the subject of this study, have no proven historical records of satisfactorily correlating to field cracking performance [11], [12], [30], [33], [35]–[38].

2.4. Summary

In this chapter, a review of the literature and technical standards was completed, namely addressing the following key aspects:

- **Reflective Cracking Phenomenon:** Reflective cracking is a common distress in HMA overlays placed over an existing cracked or jointed pavement, this phenomenon is produced by a joint effect of traffic loads and temperature changes that generate vertical and horizontal movements in the pavement structure. The mechanistic approach of this phenomenon has been proposed by some researchers in order to explain, study and control this distress. Additionally, a summary of the control techniques available in the literature to reduce or prevent the reflective cracking in asphalt pavement were also presented.
- **Asphalt Binder Cracking Evaluation:** A description of the most common methodologies for evaluating the asphalt-binder response to cracking performance and some relevant specifications were presented. Two asphalt binder tests were presented and analysed, namely (a) BBR, and (b) ER defined by the ASTM 6648 and the ASTM 6084 standards, respectively.
- **HMA Cracking Evaluation:** A description of different test methods proposed in the literature to evaluate the cracking potential of HMA in the laboratory were presented.

CHAPTER 3

EXPERIMENTAL DESIGN PLAN

The experimental design plan is presented and discussed in this section, including the asphalt concrete mixes used, the road test sections in service and their pavement structures. HMA mix data includes materials and mix design features. Characteristic field data, such as weather, traffic and pavement conditions, are also discussed.

A schematic of the experimental design plan is illustrated in Figure 4. The first step of the study was to determine and quantify the asphalt-binder low-temperature rheological properties using the BBR, ER (ductility) tests and the HMA fracture properties using the M-OT test. All the test data (asphalt-binders and HMA) were obtained from the DSS [61], [62]. The second step was to correlate the asphalt-binder low-temperature properties to the HMA fracture parameters. Lastly, a correlation of the asphalt-binder low temperature properties and HMA fracture parameters to field reflective cracking performance was executed to establish which asphalt-binder and HMA parameter(s) provided the best statistical correlation. Like the laboratory test data for asphalt-binders and HMA mixes, all the field cracking performance data was obtained from the DSS [61].

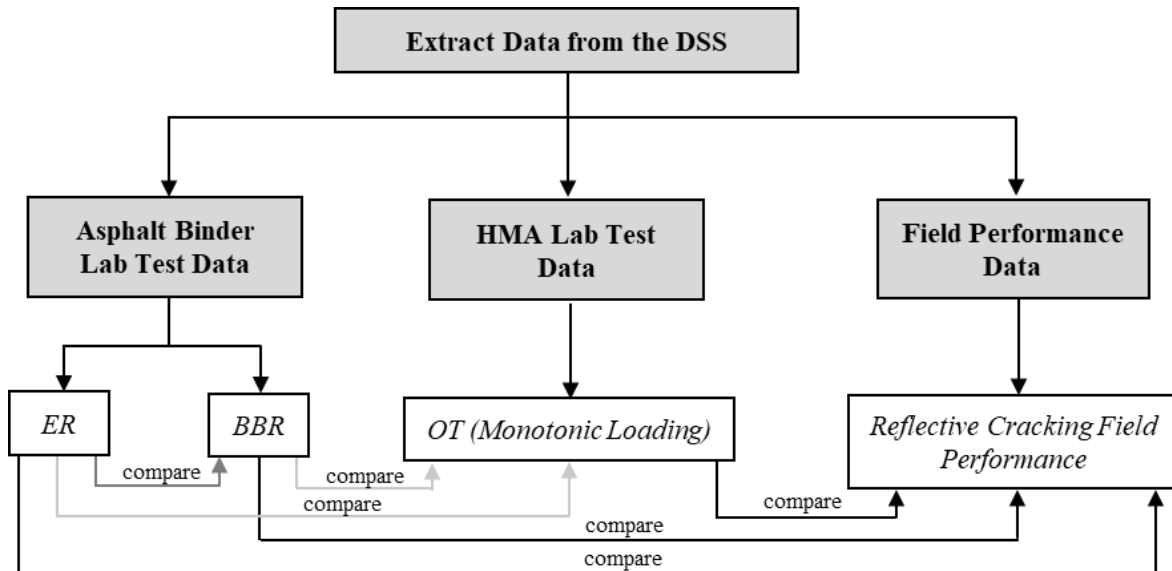


Figure 4 Schematic Illustration of the Experimental Design Plan.

From Figure 4, it is evident that the study plan incorporated various comparisons and correlations that includes the following aspects: ER versus BBR, ER versus M-OT, ER versus field cracking performance, BBR versus M-OT, BBR versus field cracking performance and M-OT versus field cracking performance. All the data for these correlative comparisons was obtained from the DSS [61], [62]. The subsequent subsections provide a description of the DSS, laboratory test methods, analysis models, the HMA mixes used, the highway test sections, and the pavement structures. The HMA mix data includes materials and mix-design characteristics. Field characteristic data such as climate, traffic, and pavement conditions are also discussed.

3.1. Texas Data Storage System (DSS)

The Texas flexible pavements and overlays database, namely the Texas Data Storage System (denoted as the DSS) developed during the Collection of Materials and Performance Data for Texas Flexible Pavements and Overlays Project (Project 0-6658) performed in cooperation with the Texas Department of Transportation (TxDOT) and the Federal Highway Administration (FHWA) in 2010 was the primary data source for this study, that is, both of the laboratory tests and field performance data used in this study.

The DSS was managed and maintained in the user-friendly and readily accessible Microsoft Access® platform with the objective to develop a comprehensive data storage system where the collected data can be efficiently stored and easily/readily accessed. This data base serves as an ongoing long-term database for Texas flexible pavements and overlays. To date, the DSS comprise of 115 in-service highway test sections with comprehensive laboratory and field performance data that includes design, construction, layer material properties (both laboratory and field measured), traffic, climate, existing distresses (in case of overlays), and field performance data – that has been routinely collected since 2010 [61], [62].

The layer material properties in the Texas DSS, among others such as HMA modulus, viscoelastic, permanent deformation, etc., include the laboratory measured HMA fracture properties from the monotonic-loading OT test – which is the subject of this document. And field performance data, among other distresses such as rutting, roughness, aggregate loss, etc., include reflective cracking (for overlay sections) that is evaluated bi-annually. Traffic measurements include vehicle counts, vehicle speed, vehicle classification, and vehicle weights using pneumatic tube counters and portable weigh-in-motion (WIM) systems. Climatic data include temperature measurements, namely air temperature and pavement temperatures, both on the surface and at 1-inch depth [61], [62].

3.2. Materials and HMA Mix-Designs

Two commonly used Texas overlay HMA mixes, namely Type C and Type D, with four different mix-designs were selected from the DSS for evaluation in this study [61], [62]. As shown in Table 1, the HMA mixes have been used as overlays on in-service highways – thus, facilitating a direct correlation of their laboratory OT cracking test results with their actual in-situ field cracking performance [61], [62].

Table 1 Asphalt-Binders and HMA Mix-Design Characteristics.

Mix Type	NMAS (Grad.)	HMA Mix-Design Characteristics			Hwy
		Asphalt-Binder		Aggregates	
C	18.75 mm (Coarse-graded)	4.9%	PG 70-22 _c	+ Limestone/dolomite+19.8% RAP	SH 358
D ₁	12.50 mm (Fine-graded)	5.1%	PG 64-22 _{d1}	+ Quartzite+20.1% RAP (10.2% coarse +9.9% fine)	US 59
D ₂	12.50 mm (Fine-graded)	5.2%	PG 64-22 _{d2}	+ Gravel/limestone/dolomite+3% RAS	SH 95
D ₃	12.50 mm (Fine-graded)	5.4%	PG 64-22 _{d3}	+ Limestone/dolomite + 1% lime + 20% RAP	SH 44

Legend: Hwy = highway; Grad. = gradation; NMAS = nominal maximum aggregate size; RAP = recycled asphalt pavement; RAS = recycled asphalt shingles

As can be seen in Table 1, the aggregate gradations comprise of three fine-graded Type D mixes (12.5 mm NMA) with one coarse-graded Type C mix (18.75 mm NMA). The HMA mix-design volumetric comprise of 4.9 to 5.4% asphalt-binder content, mostly PG 64-22 (Fine Graded - Type D mixes) and one PG 70-22 (Coarse Graded - Type C mix). The aggregates include limestone, dolomite, quartzite, and gravel with RAP (Recycled Asphalt Pavements) and RAS (Recycled Asphalt Shingles). This difference in material composition inherently allowed to evaluate the impacts of mix-design volumetric and HMA mix types.

OT testing of the HMA mixes listed in Table 1 was based on plant-mix materials collected directly from the job construction sites [61]. All the HMA samples were molded and fabricated to a target density of $93\pm 1\%$ (i.e., $7\pm 1\%$ air voids) using the Superpave gyratory compactor (SGC) [19,33]. A minimum of three sample replicates were fabricated and tested per mix type. As previously stated, the Texas DSS served as the primary data source for this study, and the mixes listed in Table 1 were strategically selected to cover only HMA mixes that are typically used for overlay and exposed to reflective cracking.

3.3. Highway Test Sections and Field Characteristics

Based on extracts from the DSS, the field characteristics of the overlaid highway sections, averaging 500 ft in length, are summarized in Table 2. While the HMA thickness is mostly 2-inches, it is clearly evident from Table 2 that the overlays are subjected to different environmental and traffic loading conditions. This diverse array of field conditions gives an opportunity to evaluate the influence of climate, temperature, and traffic loading on the predictive performance potential of the monotonic-loading OT test. For instance, the same HMA mix used on the same highway, but different lane directions, is subjected to different traffic loading – see Table 2. Thus, it was prudent in this study to assess if the laboratory test methods can capture these effects.

Table 2 Highway (Overlays) Test Sections.

Section ID (Hwy)	District (County)	Lane (Dir.)	HMA Mix Type	Overlay Thickness (Inches)	Const. Year	Climate (Temp °F)	Traffic D-ESALs (Speed)
TxDOT-TTI_00001 (US 59)	Atlanta (Panola)	Outside (SB)	D ₁	2	2011	WC (80.1)	2 380 (69.0 mph)
TxDOT-TTI_00073 (US 59)	Atlanta (Panola)	Inside (SB)	D ₁	2	2011	WC (80.1)	450 (71.3 mph)
TxDOT-TTI_00024 (SH 95)	Yoakum (Lavaca)	Outside (SB)	D ₂	3	2013	WW (90.5)	455 (65.1 mph)
TxDOT-TTI_00044 (SH 95)	Yoakum (Lavaca)	Outside (NB)	D ₂	3	2013	WW (90.5)	496 (68.7 mph)
TxDOT-TTI_00026 (SH 358)	Corpus (Nueces)	Outside (EB)	C	2	2012	M (84.5)	85 (39.5 mph)
TxDOT-TTI_00069 (SH 44)	Corpus (Jim Wells)	Outside (EB)	D ₃	2	2014	M (88.7)	325 (70.1 mph)

Legend: Const. = construction; Corpus = Corpus Christi district; D-ESALs = average daily 18-kips equivalent single axle loads; Dir = direction; Hwy = highway; M = moderate; Speed = average vehicle speed (mph); Temp = average yearly (fall & spring) temperature; WC = wet-cold; WW = wet-warm

Similarly, having two overlay thickness values (i.e., 2 and 3 inches, respectively) in the study matrix allowed to substantiate the impact and significance of the laboratory sample dimensions (thickness) on field cracking performance – especially considering that the conservativeness of the OT sample thickness at 1.5 inches. However, this is not to discount the interactive influence of other field conditions such as traffic loading, climatic variations, construction, pavement structure, existing pavement condition prior to overlay, etc.

3.4. Pavement Structures and Existing Distress Conditions

Table 3 details the pavement structures corresponding to the highway test sections used in this study. Table 5 also includes the existing cracking condition of the 500 ft long highway sections prior to HMA Overlay placement.

Table 3. Highway Pavement Structures.

Item	US 59 (Atlanta)	SH 95 (Yoakum)	SH 358 (Corpus)	SH 44 (Corpus)
HMA overlay (Year of construction)	2-inch thick Type D ₁ mix (2011)	3-inch thick Type D ₂ mix (2013)	2-inch thick Type C mix (2012)	2-inch thick Type D ₃ mix (2014)
Existing pavement structure prior to overlay	11.5-inch old HMA 16-inch LFA-treated base Subgrade	6-inch old HMA 6-inch concrete 10-inch Flex base Subgrade	6.5-inch old HMA 10-inch Flex base Subgrade	7.5-inch old HMA 6-inch Flex base Subgrade
Existing cracking distresses prior to Overlay	Transverse Alligator Longitudinal	Transverse No alligator No longitudinal	Transverse Alligator Longitudinal	Transverse No alligator Longitudinal
Existing cracking distress occurrence	Both lane directions	Both lane directions	Both lane directions	Both lane directions
Severity of transverse cracking	Moderate to high (MCW > 0.25 inches) (LTE = 57.80%)	Moderate to high (MCW > 0.25 inches) (LTE = 54.30%)	Moderate to high (MCW > 0.25 inches) (LTE = 60.01%)	Moderate to high (MCW > 0.25 inches) (LTE = 69.51%)
Other distresses prior to Overlay	Rutting (0.13 inches)	Rutting (0.58 inches)	Rutting (0.29 inches)	Rutting (0.23 inches)

Legend: Corpus = Corpus Christi district; LFA = Lime fly-ash; MCW = Mean crack width; LTE = Load transfer efficiency

As evident in Table 3, all the selected highway test sections exhibited moderate to high transverse cracking prior to HMA overlay construction – which eventually manifests as reflective cracking through the HMA overlay [61]. On average, about 32 transverse cracks were quantitatively counted at an average spacing of 15.6 ft, with an average length of 9 ft and mean crack width exceeding 0.25 inches, were counted over each of the 500 ft long highway test sections [61].

Similarly, the load transfer efficiency (LTE), determined based on falling weight deflectometer (FWD) measurements over the transverse cracks, had decayed to an average value of 60.4%, with the least being 54.3% for SH 95 [61]. With mean crack widths exceeding 0.25 inches, the overall degree of distress severity (transverse cracking) on all the

four highways was rated as moderate to high and mandated for maintenance/rehabilitation (*M&R*) works with HMA overlay placement, as indicated in Table 3, as the implemented *M&R* option.

As evident in Table 3, surface rutting averaging 0.31 inches was also measured, with highway SH 95 (at 0.58 inches) exceeding the 0.5-inch terminal threshold– which also called for *M&R* [61].

3.5. Summary

This chapter presented and discussed the experimental design plan, including the asphalt concrete mixes used, the road test sections in service and their pavement structures. HMA mix data includes materials and mix design features. Characteristic field data, such as weather, traffic and pavement conditions, were also discussed. The data collection plan included the following key aspects:

- Four Asphalt-Binders and HMA Mix-Design Characteristics were presented, these comprise: (i) three fine-graded (Type D) and one coarse-graded (Type C) mixes gradation and (ii) asphalt-binder content between 4.9 to 5.4%.
- Six overlays Test Sections in four highways were presented, these six sections include thickness values between 2 and 3 inches.
- Additionally, the pavement structures and existing distress condition were presented, including Existing pavement structure prior to overlay, Existing cracking distresses prior to Overlay, Severity of transverse cracking and other distresses prior to Overlay.

CHAPTER 4

LABORATORY TEST RESULTS AND ANALYSIS

4.1. Asphalt Binder Laboratory Test Results

4.1.1. Elastic Recovery (ER)

The ER test was performed using a ductilometer according to the ASTM 6084 [21] standard specification. The asphalt-binder specimens (three replicates per asphalt-binder) were conditioned in a 10°C water bath for one hour. Thereafter, the asphalt-binder specimens were elongated at a constant rate of 5 cm/min until reaching a fixed elongation of 20 cm, which classifies this test as a displacement-controlled, and held in this position for 5 min. Subsequently, the specimens were cut at the midpoint into two halves, left undisturbed, and allowed to be in the water bath for recovery. After an hour, both of the halves are carefully adjusted to touch each other to make the measurement of the total length of the specimen and determine the percent of elastic recovery. The ER test set up configuration and asphalt-binder specimens before and after testing, as conducted during the DSS study, are shown in Figure 5 [61], [62], [64]. The equation for computing recovered elasticity (%) is presented in the Eq. 1 in Table 4 [21].

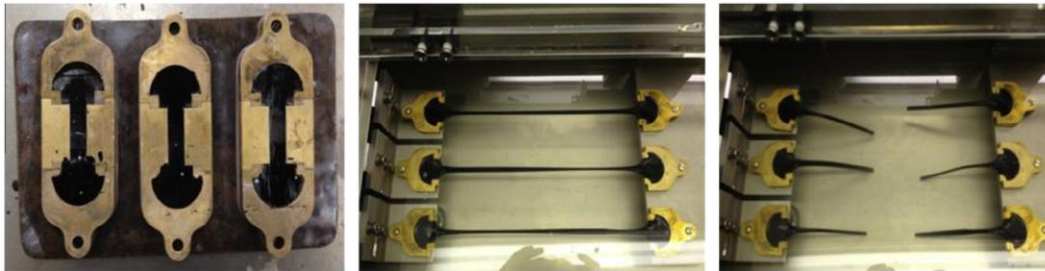


Figure 5 Elastic recovery test: (a) asphalt-binder specimen; (b) sample after 20 cm elongation; (c) sample cut in the midpoint and resting.

Table 4. Data Analysis Models for ER.

Test	Parameter	Analysis Model	Equation Number	Variable Definitions
ER (Asphalt-Binder)	<i>Recovered Elasticity (%)</i>	$\frac{E - X}{E} \cdot 100$	(Eq. 1)	E = original elongation of the specimen, cm X = elongation of the specimen, at the completion of the specified recovery time, with severed ends just touching, cm.

Table 5 summarizes the ER test results of the asphalt-binders as extracted from the DSS, which was performed using a ductilometer based on the ASTM 6084 test procedure [21], [61], [62].

Table 5. Asphalt-Binder ER Test Results.

Asphalt-Binder	Recovered Elasticity, <i>ER</i> [%]	HMA Mix (Hwy)
PG 64-22 _{d1}	23.4% (2.0%)	Type D ₁ (US 59)
PG 64-22 _{d2}	23.0% (2.8%)	Type D ₂ (SH 95)
PG 70-22 _c	52.0% (N/A)	Type C (SH 358)
PG 64-22 _{d3}	50.0% (2.6%)	Type D ₃ (SH 44)

Note: Hwy = Highway. The test results represent an average of the asphalt-binder specimen replicates evaluated. Numbers in parentheses represent the COV.

It is theoretically expected that the higher the *ER*% (ductility) of the asphalt-binder, the better the resistance to cracking [43]. Therefore, the rank order of superiority of the asphalt-binders based on the ER test results is as follows: PG 70-22_c > PG 64-22_{d3} > PG 64-22_{d1} > PG 64-22_{d2}. Statistically, PG 70-22_c (*ER* = 52%) and PG 64-22_{d3} (*ER* = 50%) are quantitatively indifferent and so are PG 64-22_{d1} (*ER* = 23.4%) and PG 64-22_{d2} (*ER* = 23%). Of interest is the quantitative difference of PG 64-22_{d3} (*ER* = 50%) from the other two PG 64-22 asphalt-binders (*ER* \cong 23.25), which is almost twice. As listed in Table 2, this difference in the ER performance is obviously related to the differences in the asphalt-binder sources and suppliers.

In terms of test data variability based on three replicate specimens per asphalt-binder, it is noted that the ER test yielded a good statistical credibility in the ER tests with COV values averaging 2.50%. As reported in the literature and considering the homogeneity nature of the asphalt-binders, these statistical results (i.e., very low COV values less than 10%) were theoretically not unexpected [17], [43], [65]. However, it is important to note that, the proximity of the average values, i.e., PG 64-22_{d1} versus PG 64-22_{d2} and PG 70-22_c versus PG 64-22_{d3}, might suggest a shortcoming in the ability of the ER test to effectively differentiate and statistically discriminate among the different asphalt-binders from different sources and suppliers. However, another hypothesis is that there are no major differences among those particular sources and suppliers.

4.1.2. Bending Beam Rheometer (BBR)

According to ASTM 6648, the original BBR setup is a three point beam bending test used to measure the mid-point deflection of a simply supported prismatic beam of asphalt-binder subjected to a constant load applied to its mid-point [20], [61], [62]. Due to the general complexity (i.e., specimen preparation, test setup, etc.) of the BBR test and the fact that the test is historically known to be a repeatable test (with coefficient of variation [COV] values generally less than 10%), only one specimen replicate was tested per asphalt-binder [61], [62].

From the data acquisition system, a curve of applied load and measured deflection at mid-point can be obtained. This curve allows to calculate the measured *stiffness* and *m-value* (slope) of the test specimen at loading times of 8, 15, 30, 60, 120, and 240 seconds [61], [62].

The *stiffness* is defined as the ratio obtained by dividing the measured maximum bending stress by the maximum measured bending strain. This parameter has been used historically in asphalt technology [20]. The *m-value* is defined by the ASTM 6648 [20] as the absolute value of the slope of the logarithm of the stiffness curve versus the logarithm of time. The graphical definition of this parameter is presented in Fig. 3 [24], [61], [62]. The analysis models for computing the *stiffness* and the *m-value* are listed in Table 6 (Eq. 2 and Eq. 3) [30], [38], [66]

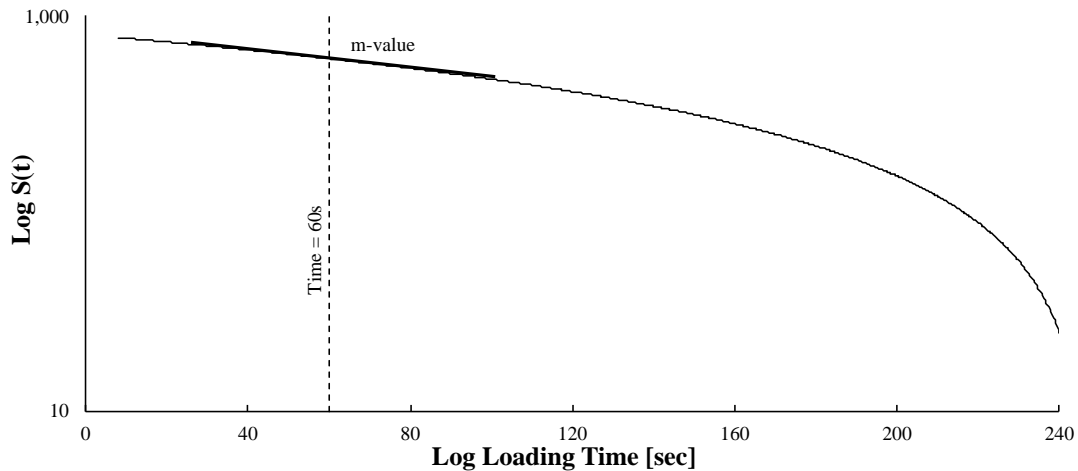


Figure 6. BBR definition of the m-value.

Table 6. Data Analysis Models for BBR.

Test	Parameter	Analysis Model	Equation Number	Variable Definitions
BBR (Asphalt-Binder)	<i>Stiffness (S)</i>	$\frac{PL^3}{4bh^3\delta(t)}$	(Eq. 2)	P = measured test load, mN L = span length, mm b = width of test specimen, mm h = depth of test specimen, mm $\delta(t)$ = deflection of test specimen at time t.
	<i>m-value</i>	$\frac{d\log[S(t)]}{d\log(t)}$	(Eq. 3)	t = loading time

Based on the DSS work plan [61], the BBR test was conducted at -12 °C and -18 °C according to the ASTM 6648 standard procedures and specifications [20]. Table 7 presents the average *stiffness (S)* and *m-value* results extracted from the DSS. Theoretically, the higher the *m-value*, the better the cracking resistance potential of the asphalt-binder and vice versa for the *S* parameter.

Table 7. Asphalt-Binder BBR Test Results.

Asphalt-Binder	BBR @ -12 °C		BBR @ -18 °C		HMA Mix (Hwy)
	<i>m-value</i>	Stiffness, <i>S</i> (MPa)	<i>m-value</i>	Stiffness, <i>S</i> (MPa)	
PG 64-22 _{d1}	0.38	80.6	0.33	196.5	Type D ₁ (US 59)
PG 64-22 _{d2}	0.39	76.8	0.33	183.0	Type D ₂ (SH 95)
PG 70-22 _c	0.37	137.0	0.30	335.0	Type C (SH 358)
PG 64-22 _{d3}	0.39	102.0	0.30	158.8	Type D ₃ (SH 44)

Note: Hwy = Highway. The test results represent an average of the asphalt binder sample replicates evaluated.

Based on the BBR test conducted at -12 °C, the ranking obtained with the *m-value* is as follows: PG 64-22_{d2} and PG 64-22_{d3} > PG 64-22_{d1} > PG 70-22_c, and PG 64-22_{d2} (lowest *S* value) > PG 64-22_{d1} > PG 64-22_{d3} > PG 70-22_c (highest *S* value) for the stiffness ranking, which is opposed to the ER ranking (Table 4). However, using the ASTM 6373 [47] criteria, *S* should not exceed 300 MPa (i.e., $S \leq 300$ MPa) and the *m-value* must be at least 0.30 (i.e., $m\text{-value} \geq 0.30$), respectively. Thus, all the asphalt-binders would be judged as acceptable at this temperature (-12 °C).

If the BBR test conducted at -18 °C is considered, the *m-value* ranking is as follows: PG 64-22_{d1} and PG 64-22_{d2} > PG 64-22_{d3} and PG 70-22_c, with all the asphalt-binders passing the ASTM 6373 acceptability criteria for this parameter, but with PG 64-22_{d3} and PG 70-22_c being on the borderline (i.e., $m\text{-value} = 0.30$). The stiffness ranking (lowest to highest *S* value) at -18 °C is PG 64-22_{d3} > PG 64-22_{d2} > PG 64-22_{d1} > PG 70-22_c. In this particular case, however, the PG 70-22_c asphalt-binder (which is the stiffest with $S = 335$ MPa) fails the ASTM 6373 criteria, i.e., $S \leq 300$ MPa [47], [52], which again is the opposite of the ER results. It is also worth noting that the PG 70-22_c, as theoretically expected, is the stiffest asphalt-binder with the highest *S* values at both temperatures.

It is important to note that the rankings at the two test temperatures, although both rank the PG 70-22_c as the poorest, show different rankings for the PG 64-22 asphalt-binders. In theory, since the asphalt-binders have the same lower temperature PG grade (i.e., -22), they should ideally exhibit low-temperature properties that are not quantitatively very different. This could partially be attributed to the differences in the source/suppliers and the viscoelastic nature of the asphalt-binders. It is, therefore, apparent that these differences may not be effectively captured by the PG classification system.

As previously mentioned, only one specimen replicate was tested per asphalt-binder for the BBR test, primarily due to the fact that the BBR test is historically known to be a repeatable test, with COV values generally less than 10% [61], [62]. So, for resource optimization purposes, only one specimen was tested for the asphalt-binders. Therefore, no COV computations were performed or reported in Table 7.

4.2. Hot Mix Asphalt Laboratory Test Results

Similar to the Texas standardized Tex-248-F [63] test method for the dynamic-loading OT test, the monotonic-loading OT protocol uses the same test setup, which consists of two plates – one fixed and one free, so that it can move horizontally to simulate the movement of joints or cracks underneath an overlay [13], [35]. However, unlike with Tex-248-F test specification [63], horizontal ram movement is unidirectional in the case of the monotonic-loading OT test [63], [67]. The monotonic-loading OT test setup, as conducted during data generation for the DSS, is schematically illustrated in Figure 7 [61].

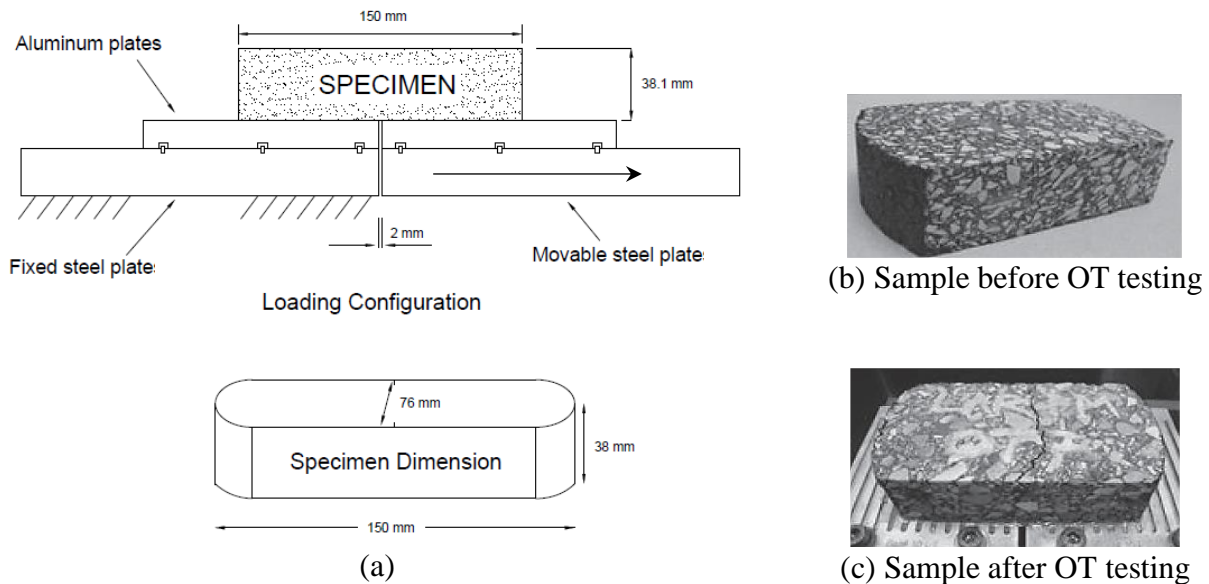


Figure 7. Monotonic-Loading OT Test Setup.

As illustrated in Figure 7, the ram movement is unidirectional for the movable steel plate. Consistent with the Tex-248-F specification [9], the HMA sample dimensions are 6 inches (150 mm) in length, 3 inches (75 mm) wide, and 1.5 inches (37.5 mm) thick [68]. For statistical credibility, a minimum of three sample replicates must be tested per mix type per test condition [30]. As documented in Walubita et al. [30] and the DSS [61], the work reported in this document is based on a monotonic loading rate of 0.125 in/min at 25°C (77 °F) until complete crack failure. During monotonic OT testing, the key output data is the load-displacement (L-D) response curve, which is exemplified in Figure 8.

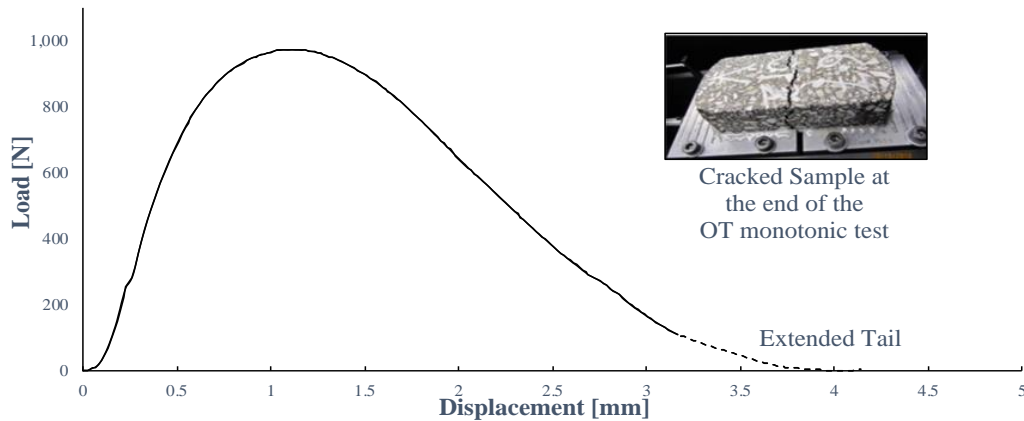
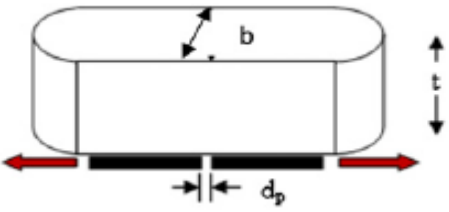


Figure 8 Monotonic-Loading loading OT L-D Response Curve [30].

Note that during monotonic-loading OT testing, it is important to always terminate the test only after the load has completely dropped to zero so as to get a full L-D response curve. A full L-D response curve enables accurate and representative modeling of the HMA fracture behavior as well as computation of the corresponding HMA fracture parameters including the area under the curve – otherwise, approximate tail extending, as exemplified in Figure 8, would be an optional estimate [30].

From the L-D data, various HMA fracture parameters are then calculated, namely the following: tensile strength (σ_t); the tensile strain at peak failure load (ϵ_t); the stiffness or tensile modulus (E_t); the fracture energy (FE , sometimes called G_f , which is the area under the L-D response curve); and the fracture energy index ($FE Index$). The mathematical models for computing these HMA fracture parameters are listed in Table 8 [30], [38], [66].

Table 8. Data Analysis Models for M-OT.

Test	Parameter	Analysis Model	Equation Number	Variable Definitions
M-OT	Tensile Strength (σ_t)	$\frac{P_{max}}{tb}$	(Eq. 4)	P_{max} = Maximum peak load at sample failure b = OT sample width t = Sample thickness D_0 = Displacement at the start of the test D_p = Displacement at peak load 
	Tensile Strain (ϵ_t)	$\frac{D_p - D_0}{D_p}$	(Eq. 5)	
	Tensile Modulus (E_t)	$\frac{\sigma_t}{\epsilon_t}$	(Eq. 6)	
	Fracture Energy (FE)	$\frac{1}{tb} \int f(x)dx$	(Eq. 7)	
	Fracture Energy Index ($FE Index$)	$\frac{FE}{t \cdot \sigma} \cdot \epsilon \cdot 10^3$	(Eq. 8)	

In monotonic-loading cracking tests of this nature, the maximum load at sample failure or peak load is typically used as an indicative parameter to characterize the crack resistance potential of HMA [66]. As noted by Lee et al. [66], however, the resultant tensile strength, which is calculated as a function of the peak load, is not considered a good fracture parameter

to represent, by itself, the cracking resistance potential of the HMA mixes. This is because (like the peak failure strain), the tensile strength is a single-point parameter and does not take into account the full loading history endured by the HMA sample [66]. However, Kim et al. [69] reported that fracture energy (FE) determined at 20°C (68 °F) was a good indicator of a mix's fracture resistance relative to the field performance data. In lieu of the tensile strength, Kim et al. [69] recommended the FE as the fracture parameter to use for quantifying the cracking resistance potential of HMA mixes. From Table 8, note that FE is essentially the mathematical computation of the integral area under the L-D response and therefore, captures the full-loading history and fracturing endured by the HMA sample.

Fracture energy index ($FE Index$), which is a composite function of the tensile strength, failure strain, and FE , has also proved to be effective in capturing the complete loading history and fracturing of the HMA sample and therefore, the crack resistance potential of the HMA mix in the laboratory [66]. In comparison to the FE , the $FE Index$ is a dimensionless parameter and more convenient to use for differentiating mixes. However, the $FE Index$ is a relatively newly formulated HMA fracture parameter and as such, it lacks historical documentation on any correlations nor validation with field cracking performance data [30], [35], [66].

Table 9 presents the HMA fracture parameters (an average of three replicate samples) and COV results determined from monotonic-loading OT output data. The HMA fracture parameters were computed using the equations/models listed in Table 8 and include the following: peak load, tensile strength (σ_t); the tensile strain at peak failure load (ϵ_t), the stiffness or tensile modulus (E); the fracture energy (FE , sometimes called G_f), and the $FE Index$.

Table 9. Monotonic Overlay Test Results.

HMA Mix (Table 3)	Peak Load, P_{max} [lbs]	Tensile Strength, σ_t [psi]	Tensile Strain, ϵ_t [in/in]	Tensile Modulus, E [psi]	Fracture Energy, FE [J/m ²]	Fracture Energy Index, $FE Index$
Type D ₁ (US 59)	858 (7.1%)	191 (7.1%)	0.17 (6.7%)	1103 (16.1%)	1555 (12.4%)	5.43 (17.2%)
Type D ₂ (SH 95)	439 (6.2%)	97 (6.2%)	0.19 (21.1%)	535 (23.6%)	660 (7.0%)	4.95 (28.8%)
Type C (SH 358)	696 (15.0%)	155 (15.0%)	0.13 (4.3%)	1155 (15.4%)	533 (13.7%)	1.76 (3.7%)
Type D ₃ (SH 44)	525 (9.3%)	117 (9.3%)	0.15 (20.8%)	783 (24.8%)	809 (8.6%)	4.10 (22.2%)

Note: The test results represent an average of at least three HMA simple replicates
Numbers in parentheses represent the COV percentages for each HMA fracture parameter.

From Table 9, the ranking of the HMA mixes based on the magnitude of the peak load is Type D₁ (858 lbs) > Type C (696 lbs) > Type D₃ (525 lbs) > Type D₂ (439 lbs). The tensile strength is primarily calculated as a function of the peak load and so, it provides the same ranking as the peak load, namely: Type D₁ (191 psi) > Type C (155 psi) > Type D₃ (117 psi) > Type D₂ (97 psi). Borrowing from the Texas Tex-226-F criteria of 85-200 psi for mix acceptability in terms of the tensile strength [70], all the HMA mixes in Table 9 would be

judged as acceptable – although mix Type D₂ (at 97 psi) is close to the 85 psi lower borderline. Note that based on the Tex-226-F criteria, a tensile strength value less than 85 psi is theoretically indicative of a soft and probably unstable mix, which would have a challenge to simultaneously balance and meet the HMA rutting requirements, particularly at elevated service temperatures [70]–[72]. A tensile strength exceeding 200 psi, on the other hand, is theoretically/quantitatively considered to be indicative of a stiff-brittle mix, which is not good for HMA cracking resistance performance [71], [72].

The mix ranking based on the tensile strain magnitude (Table 9) is Type D₂ (0.19 in/in) > Type D₁ (0.17 in/in) > Type D₃ (0.15 in/in) > Type C (0.13 in/in); which is different from the peak load and tensile strength rankings. In general, a high failure tensile strain is theoretically desired for good cracking resistance potential – but, again, not too high (say greater than 0.50 in/in) as it might theoretically indicate an unstable soft mix susceptible to rutting. A low failure tensile strain, say less than 0.10 in/in, could theoretically imply an undesirable stiff-brittle mix susceptible to cracking [71], [72].

The tensile modulus, which is computed as a function of the tensile strength and strain (Table 8), provides the following ranking according to Table 9: Type C (1155 psi) > Type D₁ (1103 psi) > Type D₃ (783 psi) > Type D₂ (535 psi). These results suggest that Type C, with the highest tensile modulus (1155 psi), was the stiffest mix in the study matrix. This is consistent with theoretical expectations and volumetric characteristics of Type C mix as shown in Table 1 i.e., it has the coarsest aggregate gradation (NMAAS = 18.75 mm), highest asphalt-binder PG grade (PG 70-22), lowest asphalt-binder content (4.9%), and moderately quality aggregates comprising of limestone-dolomite and RAP, which makes the HMA mix stiffer [61], [62].

For *FE* and *FE Index*, higher values are theoretically desired for good cracking resistance potential and vice versa for lower values. From Table 9, both of these HMA fracture parameters provide the same ranking of the mixes, namely: Type D₁ > Type D₂ > Type D₃ > Type C. In comparison to the previously discussed single-point parameters (i.e., P_{max} , σ_t , ϵ_t , and E_t), the *FE* and *FE Index* are mathematically considered to be more representative of the HMA cracking/fracture response-behavior as they are able to capture the full loading history and complete fracturing endured by the HMA sample during monotonic-loading OT testing (see Figure 8 and Table 8). True to this mathematical theory, both of HMA fracture parameters (*FE* and *FE Index*) rank the coarse-graded Type C as the poorest mix in the study matrix – which is in line with its (Type C) mix-design volumetrics listed in Table 1. By contrast, the fine-graded Type D₁ mix, with prime quality quartzite aggregates and PG 64-22 asphalt-binder, is ranked as the best mix in the study matrix by both the *FE* and *FE Index* parameters.

4.2.1. Statistical Analysis (ANOVA and Tukey's HSD)

In order to further analyze the potential of the HMA fracture parameters obtained from the monotonic loading OT to differentiate between the mixes evaluated, Analysis of Variance (ANOVA) and Tukey's Honestly Significant Difference (Tukey's HSD) methods was used at 95% reliability level for each respective parameter [73], [74] to evaluate if the mixtures are statistically different, understanding the variability of the data.

Tukey's Honestly Significant Difference test is a statistical tool used to determine if the relationship between two sets of data is statistically significant. This test build confidence intervals with an α level of significance for all possible pairwise comparisons. With this method we can find a test statistic that allows us to evaluate the following hypotheses:

$$H_0 : \mu_i = \mu_j \quad \text{vs.} \quad H_0 : \mu_i \neq \mu_j$$

The proposed statistical methods were performed at 95% reliability ($\alpha = 5\%$). The mixes were categorized into different statistical 'alphabetical groups' A, B, C, and D. HMA mixes in the same group have parametric values that are statistically not significantly different and vice versa, that is, those in the same alphabetical group are not statistically different. The groups are arranged in a statistical rank order of superiority as follows: $A > B > C > D$; where A is associated with HMA mixes that statistically and quantitatively represent the best fracture behavior in terms of cracking resistance in the laboratory. This statistical analysis was performed using the free-use software R, the main results are summarized in Table 10 to Table 15.

Table 10. Statistical Analysis ANOVA y Tukey's HSD for Peak Load

Comparison	Confidence Intervals for the parameter $\mu_i - \mu_j = 0$		Hypotheses Testing
			p-value
Type D ₁ -Type C	19.11	304.81	0.025
Type D ₂ -Type C	-384.81	-129.27	0.000
Type D ₃ -Type C	-298.37	-42.83	0.009
Type D ₂ -Type D ₁	-546.77	-291.23	0.000
Type D ₃ -Type D ₁	-460.33	-204.79	0.000
Type D ₃ -Type D ₂	-24.22	197.09	0.148

Table 11. Statistical Analysis ANOVA y Tukey's HSD for Tensile Strength

Comparison	Confidence Intervals for the parameter $\mu_i - \mu_j = 0$		Hypotheses Testing
			p-value
Type D ₁ -Type C	4.24	67.74	0.025
Type D ₂ -Type C	-85.51	-28.72	0.000
Type D ₃ -Type C	-66.31	-9.52	0.009
Type D ₂ -Type D ₁	-121.50	-64.71	0.000
Type D ₃ -Type D ₁	-102.30	-45.51	0.000
Type D ₃ -Type D ₂	-5.39	43.80	0.148

Table 12. Statistical Analysis ANOVA y Tukey's HSD for Tensile Strain

Comparison	Confidence Intervals for the parameter $\mu_i - \mu_j = 0$		Hypotheses Testing
			p-value
Type D ₁ -Type C	-0.03	0.11	0.400
Type D ₂ -Type C	-0.01	0.12	0.097
Type D ₃ -Type C	-0.04	0.09	0.784
Type D ₂ -Type D ₁	-0.05	0.08	0.871
Type D ₃ -Type D ₁	-0.08	0.05	0.815
Type D ₃ -Type D ₂	-0.09	0.02	0.281

Table 13. Statistical Analysis ANOVA y Tukey's HSD for Tensile Modulus

Comparison	Confidence Intervals for the parameter $\mu_i - \mu_j = 0$		Hypotheses Testing
			p-value
Type D ₁ -Type C	-460.95	357.09	0.981
Type D ₂ -Type C	-985.79	-254.12	0.001
Type D ₃ -Type C	-737.36	-5.68	0.046
Type D ₂ -Type D ₁	-933.86	-202.19	0.003
Type D ₃ -Type D ₁	-685.43	46.25	0.095
Type D ₃ -Type D ₂	-68.39	565.26	0.146

Table 14. Statistical Analysis ANOVA y Tukey's HSD for Fracture Energy

Comparison	Confidence Intervals for the parameter $\mu_i - \mu_j = 0$		Hypotheses Testing
			p-value
Type D ₁ -Type C	787.23	1258.39	0.000
Type D ₂ -Type C	-83.24	338.19	0.322
Type D ₃ -Type C	65.62	487.04	0.010
Type D ₂ -Type D ₁	-1106.05	-684.62	0.000
Type D ₃ -Type D ₁	-957.19	-535.77	0.000
Type D ₃ -Type D ₂	-33.62	331.34	0.125

Table 15. Statistical Analysis ANOVA y Tukey's HSD for Fracture Energy Index

Comparison	Confidence Intervals for the parameter $\mu_i - \mu_j = 0$		Hypotheses Testing
			p-value
Type D ₁ -Type C	1.13	6.22	0.005
Type D ₂ -Type C	0.92	5.46	0.006
Type D ₃ -Type C	0.06	4.61	0.043
Type D ₂ -Type D ₁	-2.76	1.79	0.920
Type D ₃ -Type D ₁	-3.61	0.94	0.345
Type D ₃ -Type D ₂	-2.82	1.12	0.589

Table 16 summarizes the classification in the different statistical "alphabetic groups" A, B, C and D obtained from the statistical Analysis Of Variance (ANOVA) and Tukey's HSD.

Table 16. ANOVA and Tukey's HSD Test Analyses.

HMA Mix (Highway)	Peak Load, P	Tensile Strength, σ_t	Tensile Strain, ϵ_t	Tensile Modulus, E_t	Fracture Energy, FE	Fracture Energy Index, $FE Index$
Type D ₁ (US 59)	A	A	A	A	A	A
Type D ₂ (SH 95)	C	C	A	B	B	A
Type C (SH 358)	B	B	A	A	C	B
Type D ₃ (SH 44)	C	C	A	A	B	A

Note: Statistical rank order of superiority based on the parametric magnitude = A>B>C>D

The results presented in Table 16 indicate that at 95% reliability level, only the peak load (P), tensile strength (σ_t), and fracture energy (FE) have the ability to statistically differentiate the cracking resistance potential among the tested HMA mixes into three distinctive Groups A, B, and C. By contrast, the tensile strain (with only one grouping), tensile modulus and $FE Index$ (with two groupings) are unable to fully capture any significant statistical difference among the tested HMA mixes.

The results indicate that for most of the evaluated parameters the mixes Type D₂ and Type D₃ are statistically similar, only Tensile Modulus (E) was able to differentiate them, suggesting that the Type D₃ is better than the type D₂. In the same line, all the HMA fracture parameters evaluated from the monotonic-loading OT test statistically ranks Type D₁ as the most superior mix in terms of cracking resistance potential in the laboratory, an aspect that goes according to the mix-design volumetric listed in Table 1 (i.e., fine-graded, 12.5 mm NMAS, high quality quartzite aggregates, etc.).

Although the tensile strain (ϵ_t) identifies the Type D₂ as the best performer, this parameter fails to identify any statistical difference among the other mixes, i.e., all are ranked in Group A. The superior screening capability of the peak load, tensile strength, and FE is further substantiated by their lower statistical variability in the test data, with low COV values ranging from 6.2% to 15%, as can be seen in Table 16 and Table 9. By contrast, the tensile strain, tensile modulus, and $FE Index$ exhibit comparatively higher variability with some COV values exceeding 15% and reaching as high as 28.8% – which partially negates their statistical differentiation capabilities [74].

4.3. Laboratory Test Comparisons and Rankings

As presented in the ER test case, the average m -values are very close to each other, which suggest a possible shortcoming in the ability of this parameter to statistically differentiate among the tested asphalt-binders. However, it is important to note that the asphalt-binder low temperature tests (ER and BBR) are very repeatable with very low statistical variability, i.e., low COV values than 10%. The overall ranking of the asphalt-binders and the corresponding HMA mixes are summarized in Table 17.

Table 17. Laboratory HMA and Asphalt-Binder Ranking.

Rank	M-OT						ER [%]	BBR			
	P_{max}	σ_t	ε_t	E_t	FE	FE Index		@ -12 °C		@ -18 °C	
								<i>m-value</i>	<i>S</i>	<i>m-value</i>	<i>S</i>
1	D ₁	D ₁	D ₂	C	D ₁	D ₁	C	D ₂	D ₂	D ₂	D ₃
2	C	C	D ₁	D ₁	D ₂	D ₂	D ₃	D ₃	D ₁	D ₁	D ₂
3	D ₃	D ₃	D ₃	D ₃	D ₃	D ₃	D ₁	D ₁	D ₃	D ₃	D ₁
4	D ₂	D ₂	C	D ₂	C	C	D ₂	C	C	C	C

From Table 17, asphalt-binders PG 64-22_{d1} and PG 64-22_{d2} and HMA mixes Type D₁ and Type D₂ top the list. On the other hand, asphalt-binder PG 70-22_c and the corresponding HMA Type C seems to be the poorest with seven out of the eleven (63%) parameters ranking it at the bottom. In general, both the asphalt-binder and HMA laboratory tests exhibited reasonable correlations and were in agreement with respect to the rankings. Based on the results in Table 17, the overall rank order of superiority, for both the asphalt-binders and HMA mixes, in terms of cracking resistance potential is as follows: D₁ = D₂ > D₃ > C.

4.4. Test Repeatability and Data Quality

Using a COV of 30% (i.e., $COV \leq 30\%$) as the threshold measure of test data variability and statistical acceptability [61], [62], [71], [75]. As mentioned before, it is noted that the Asphalt binder test yielded a good statistical credibility, with COV values averaging 2.50% in the ER case. As reported in the literature and considering the homogeneity nature of the asphalt-binders, these statistical results (i.e., very low COV values less than 10%) were theoretically not unexpected [17], [43], [65]. BBR and ER test is historically known to be a repeatable test with coefficient of variation [COV] values generally less than 10% [61], [62].

It is evident from Table 9 that the monotonic-loading OT is fairly a repeatable test with low variability in the test data. The quantitative values for the HMA fracture parameters in Table 9, which is an average representation of three sample replicates, all have COV values less than 30%. This indicates that the repeatability of the monotonic-loading OT test as well as the test data consistency and quality are of acceptable statistical credibility.

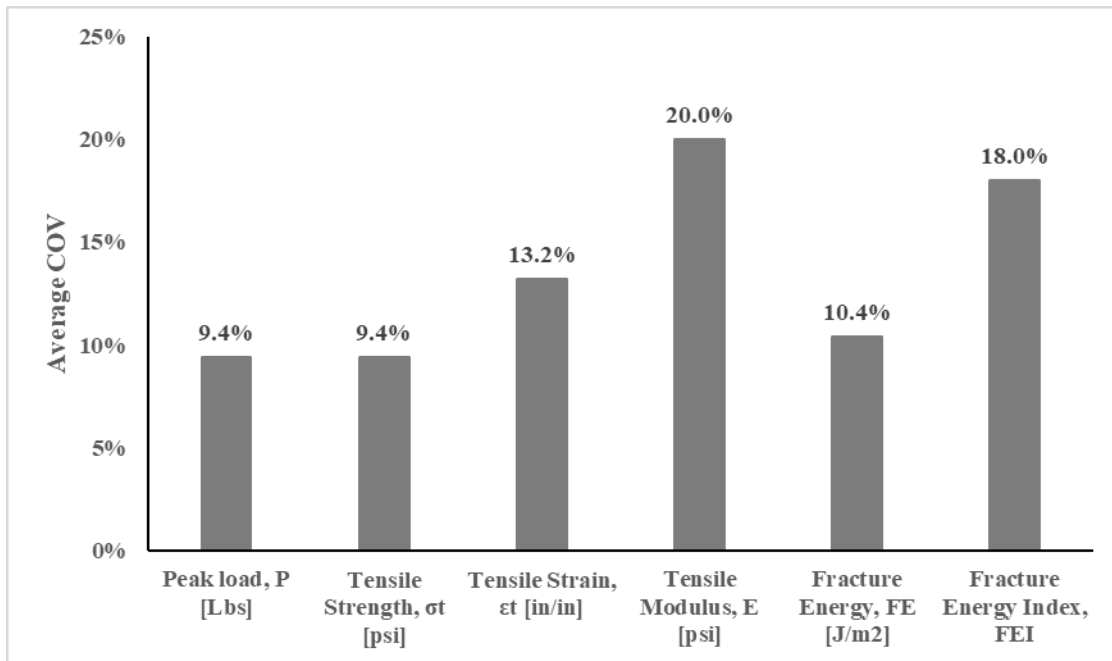


Figure 9 HMA Fracture Parameter's average COV

When comparing the individual HMA fracture parameters, it is noted the peak load and tensile strength yielded the highest statistical credibility with the lowest COV values averaging 9.40%. For the HMA mixes evaluated as listed in Table 1 tensile modulus and *FE Index* appear to be the most variable HMA fracture parameters, with the highest COV values averaging 20.0% and 18.0%, respectively – however, all are still acceptable within the 30% threshold. The tensile strain and *FE* fall in the middle, with COV values averaging 13.2% and 10.4%, respectively.

Thus, in terms of consistency and statistical credibility/confidence based on the variability, the HMA fracture parameters would be ranked as follows: (1) Peak Load and Tensile Strength ($COV_{Average} = 9.4\%$), (2) Fracture Energy ($COV_{Average} = 10.4\%$), (3) tensile strain ($COV_{Average} = 13.2\%$), (4) *FE Index* ($COV_{Average} = 18.0\%$), and (5) Tensile Modulus ($COV_{Average} = 20.0\%$).

4.5. Synthesis and Discussion

The proximity of the average values of the *Elastic Recovery* (ER) and *m-value* (BBR) and *tensile strain* (M-OT) might suggest a possible shortcoming in the ability of this parameter to statistically differentiate and statistically discriminate among the tested asphalt-binders.

In terms of test data variability based on three replicate specimens per asphalt-binder/HMA, it is noted that the ER test yielded a good statistical credibility in the ER tests with COV values averaging 2.50%, and the monotonic-loading OT is fairly a repeatable test with low variability in the test data, with COV values less than 30%; For the BBR only one specimen replicate was tested per asphalt-binder and this analysis cannot be conducted. The *Peak Load* and *Tensile Strength* obtained from the M-OT appears to be the parameters with the best consistency and statistical credibility/confidence based on the variability with COV values

lower than 10%. The *Fracture Energy Index* and *Tensile Modulus* appear to be the most variable HMA fracture parameters, with the highest COV values averaging 20.0% and 18.0%, respectively.

Analysis of Variance (ANOVA) and Tukey's Honestly Significant Difference (Tukey's HSD) methods indicate that at 95% reliability level, only the peak load (P), tensile strength (σ_t), and fracture energy (FE) have the ability to statistically differentiate the cracking resistance potential among the tested HMA mixes into three distinctive Groups A, B, and C, showing a good ability to differentiate between mixes. As expected, *Tensile Strain* was unable to capture any significant statistical difference (with only one grouping), this results could be attributed to the proximity of the average values and the high variability of the parameter.

4.6. Summary

In this chapter, the laboratory test results from the Elastic Recovery, Bending Beam Rheometer and Monotonic Overlay test were presented. An Analysis of Variance (ANOVA) and Tukey's Honestly Significant Difference (Tukey's HSD) were performed in order to evaluate and analyze the potential of HMA fracture parameters to differentiate between mixes. The key outcomes from the chapter are as follows:

- ER, BBR and M-OT test results were presented and analyzed for each of the evaluated mixes/asphalt binders.
- The ability of each HMA fracture parameters to differentiate between mixes were evaluated using the Analysis of Variance (ANOVA) and Tukey's Honestly Significant Difference (Tukey's HSD) methods.
- The repeatability and data quality of the output data were also evaluated using the COV.
- Finally, the main results were summarized, analyzed and discussed.

CHAPTER 5

FIELD PERFORMANCE RESULTS AND ANALYSIS

The field performance data of the six selected sections were obtained from the Texas Flexible Pavements and Overlays Database (DSS). Based on the DSS protocol [62], field performance monitoring and evaluation of the highway test sections is conducted bi-annually, namely: (1) just after winter to capture the low-temperature related distresses such as cracking, aggregate loss, etc., and (2) just after summer to capture the high-temperature related distresses such as rutting, bleeding, etc.

As mentioned before, this document is focus is on cracking (reflective) that was consistently measured at the same marked and GPS referenced points on the 500 ft long Overlay test sections corresponding to the same points/locations where transverse cracking had been measured/recorded prior to HMA Overlay placement.

All crack measurements were manual and walking survey-based with visual counts, measuring tapes (for crack length and spacing measurements), Vernier calipers (for crack width measurements), markers (for paint marking the test section and crack locations), GPS device (GPS coordinates for the test section and crack locations), DMI wheel (for distance measurements), and high resolution smart cameras (for taking pavement surface and crack pictures).

As per DSS protocol [62], the percentage reflective cracking ($\%RC$) is determined as a function of the number of transverse cracking that have propagated and reflected onto the HMA overlaid surface over a 500 ft long test section as illustrated in Eq. 9:

$$\%RC = 100\% \frac{nTC_R}{nTC_E} \quad (\text{Eq. 9})$$

In Eq. 9, $\%RC$ is reflective cracking, which is the percentage number of transverse cracks that have propagated and reflected onto the HMA overlaid surface over a 500 ft long test section; nTC_R is the number of transverse cracks that have reflected through and quantitatively counted over a 500 ft long HMA overlaid test section; and nTC_E is the number of quantitatively counted transverse cracks existing on the 500 ft long test section prior to HMA Overlay placement. The pavement surface conditions of the highway test sections, as of Spring 2019, are photographically shown in Figure 10.



Figure 10. Pavement Surface Condition (Spring 2019).

With the exception of TxDOT-TTI_00073 (US 59) Figure 10 shows visible surface (reflective) cracking on the pavement surface of all the highway test sections. While test sections TxDOT-TTI_00001 and TxDOT-TTI_00073 are next to each other on the same highway (US 59), test section TxDOT-TTI_00073 is located in the inside lane with very little truck traffic. As listed in Table 2 the daily traffic loading ESALs on the US 59 inside lane (TxDOT-TTI_00073) is only 450 versus 2380 for the outside lane (TxDOT-TTI_00001). Since the pavement structures are the same and both highway sections endure the same climatic conditions, it is most likely that the cause of the differences in the reflective cracking performance could be attributed to traffic loading – especially considering that the two highway test sections were constructed at the same time by the same contractor using a similar construction method [61].

Appendix A shows the results of the field measurements reported in the Texas Flexible Pavements And Overlays Database (DSS), the complete information of the measured data can be seen in Appendix A, included the date of measurement; this data will allow us to make a quantitative comparison of the performance that the test sections have had against the reflection cracking phenomenon.

Figure 11 is a graphically plot of the reflective cracking performance of the highway test sections as a function of time, expressed in terms of pavement age (i.e., months). It is clear that all the test sections (TxDOT-TTI_00024 and TxDOT-TTI_00044) on highway SH 95 (with Type D₂ mix) had failed (with reflective cracking close to 100%), just after 40 months (3.33 years) of service – whilst, the rest of the highway test sections were still well below the 25%. After 85 months (7.1 years) of service, test section TxDOT-TTI_00026 (SH 358) at 25.5% reflective cracking, with Type C mix, had reached the 25% threshold, with test section TxDOT-TTI_00001 (US 59) trailing closely at 16.98%.

The cracking performance difference between the test sections on highway US 59, is yet again graphically visible, with TxDOT-TTI_0073 (inside lane) registering zero reflective cracking versus 16.98% for TxDOT-TTI_00001 (outside lane) after 85 months (7.1 years) of service life, as mentioned before, the difference can be attributed to traffic loading presented in Table 2 TxDOT-TTI_00069 (SH 44) had reflected only 8.43% of the pre-existing transverse cracks after 47 months of service.

Based on the results in Figure 11, the test sections on highway SH 95 should be scheduled for immediate *M&R* as they have exceeded the terminal criteria – whilst TxDOT-TTI_00026 should be the next in the pipeline for *M&R* scheduling. Not to discount the impacts of traffic loading, pavement structure, and climatic conditions, it is interesting to note that SH 95 with a 3-inch thick Type D₂ mix had the thickest HMA overlay (versus the rest at 2 inches), and yet, it is the test sections on this highway (SH 95) that have completely failed with reflective cracking close to 100% at the time of writing this document.

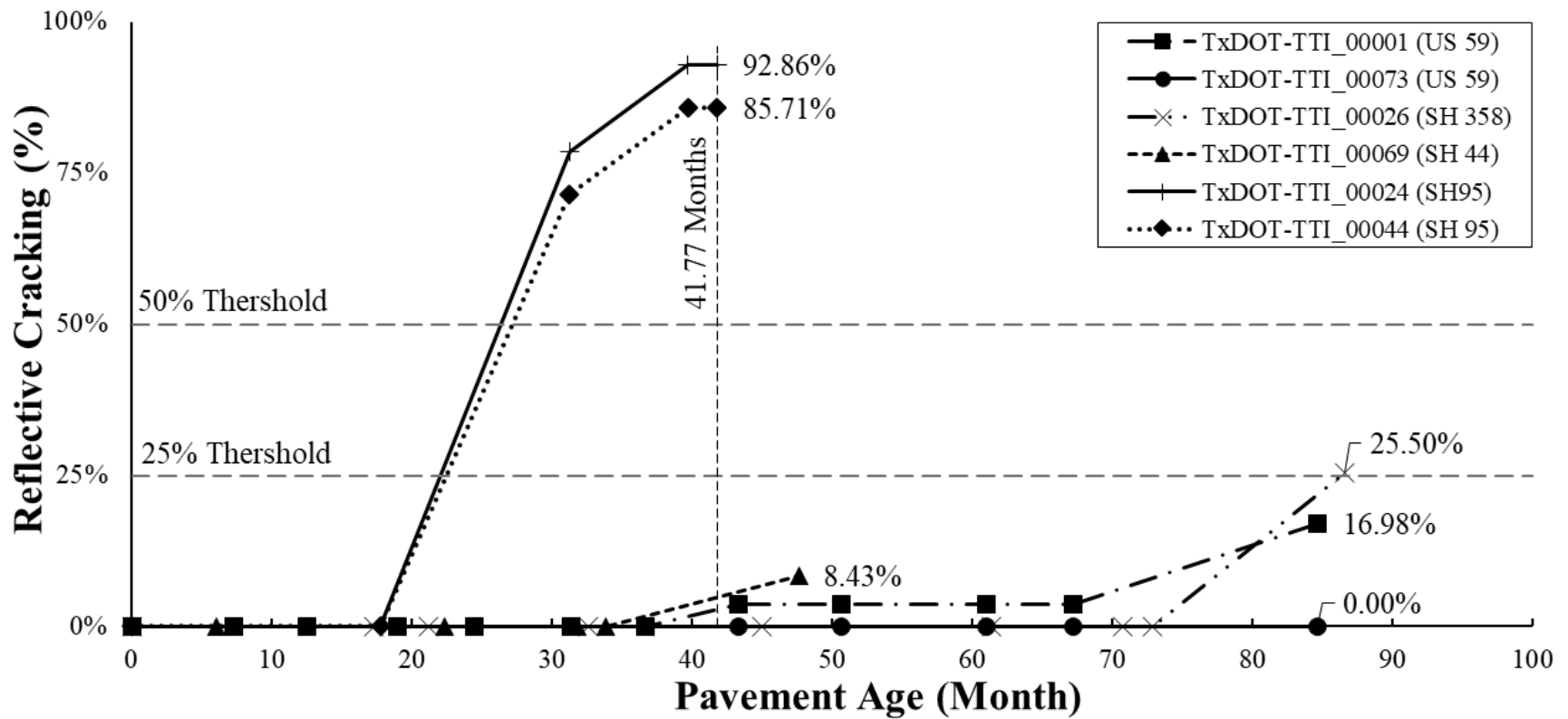


Figure 11. Reflective Cracking Performance versus Time.

If the slope of each curves in Figure 11 is assumed to represent the rate of reflective cracking performance of the test sections, in this particular case percentage of the pre-existing transverse cracks reflected to surface per year (i.e., %cracking/year), the rank order of superiority would be as follows: TxDOT-TTI_00073 (0.00% cracking/year) > TxDOT-TTI_00069 (2.43% cracking/year) > TxDOT-TTI_00001 (2.43% cracking/year) > TxDOT-TTI_00026 (4.44% cracking/year) > TxDOT-TTI_00044 (42.68% cracking/year) > TxDOT-TTI_00024 (46.24% cracking/year).

However, this analysis does not take into account the differences in traffic loading endured by each highway test section. So, to account for traffic loading and facilitate easy performance comparisons, the time stamp (horizontal X-axis) in Figure 11 was normalized to the traffic domain using the ESAL data measured from pneumatic tube counters and portable WIM units. The measured reflective cracking versus the estimated traffic ESALs in each test section are plotted in Figure 12.

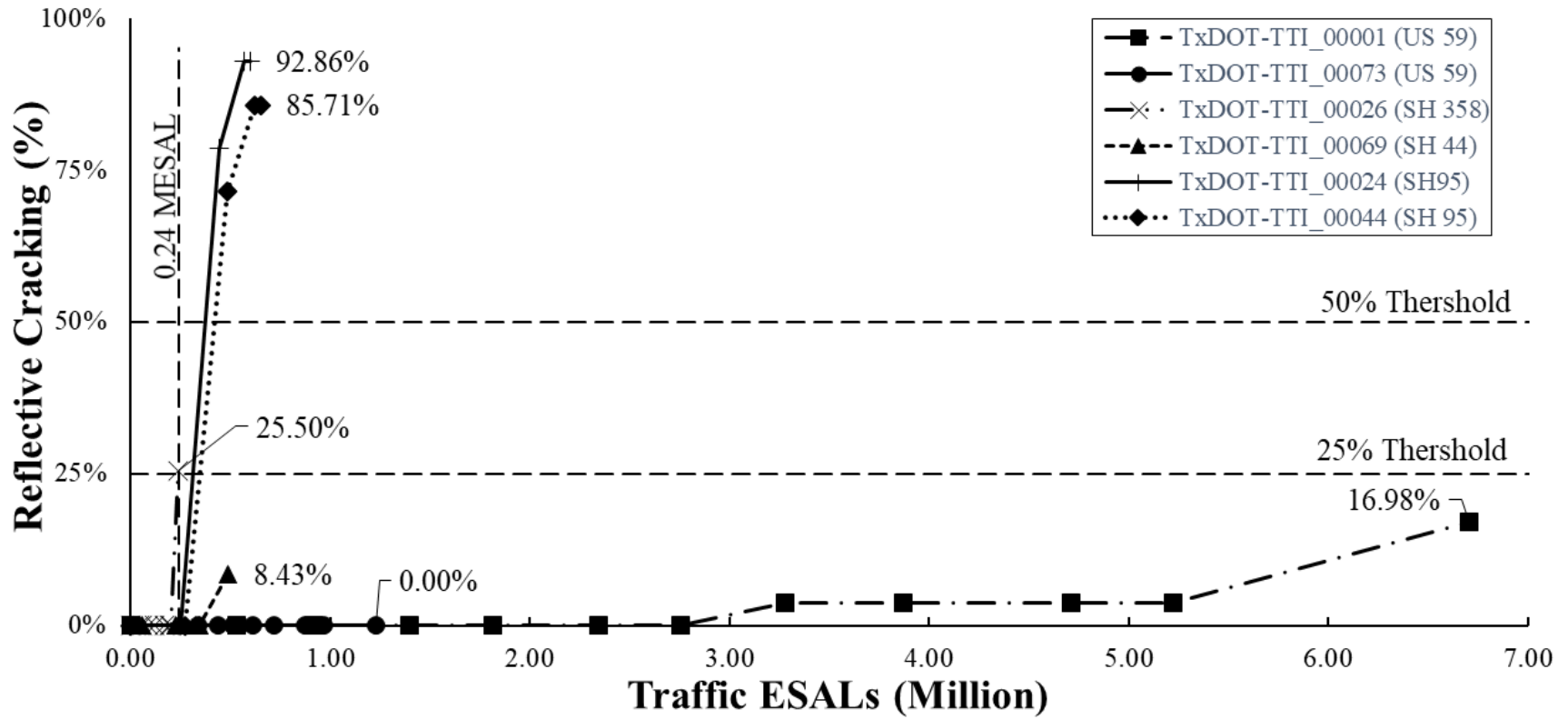


Figure 12. Reflective Cracking Performance versus Traffic Loading.

From Figure 12, the SH 95 test sections (TxDOT-TTI_00024 and TxDOT-TTI_00044) and TxDOT-TTI_00026 (SH 358), all failed and reached the terminal criteria (25% Threshold) with less than 0.50 million ESALs of traffic loading – whilst it is only 8.43% for TxDOT-TTI_00069 (SH 44). In contrast, TxDOT-TTI_00001 (US 59), which has endured the highest traffic loading, had cracked only about 16.98% after 6.71 million ESALs. Within the same time frame, TxDOT-TTI_00073 (inside lane) had endured only about 1.23 million ESALs of traffic loading (with zero reflective cracking) versus the 6.71 million ESALs for TxDOT-TTI_00001 (outside lane). By comparison, TxDOT-TTI_00001 (US 59) took about 2.75 million ESALs before cracking started to reflect on the overlay surface while TxDOT-TTI_00026, TxDOT-TTI_00024 and TxDOT-TTI_00044 started cracking just after enduring 0.20 to 0.27 million ESALs of traffic loading (i.e., 0.20, 0.25, and 0.27 million ESALs, respectively).

With the objective to rank the test section's performance, the slope of each curve in Figure 12 was estimated assuming as linear regression fit-line. The slope (R_{rc}), representing the rate of reflective cracking per traffic loading ESAL (i.e., %cracking/MESAL), was computed both for the full-curve (Slope A) and from the instance reflective cracking started (Slope B) on each test section. The higher the R_{rc} value in magnitude, the greater the propensity to reflective cracking.

Table 18. Rate of Reflective Cracking per Traffic Loading ESAL (%Cracking/MESAL).

Section ID (Hwy)	Slope A, R_{rc} (%) (Full-Curve)	Start of Cracking (ESALs [Million])	Slope B, R_{rc} (%) (From Start of Cracking)
TxDOT-TTI_00001 (US 59)	0.02 ($R^2 = 66.08\%$)	2.75	0.04 ($R^2 = 73.97\%$)
TxDOT-TTI_00073 (US 59)	0.00% (N/A)	N/A	0.00 (N/A)
TxDOT-TTI_00024 (SH 95)	1.81 ($R^2 = 85.92\%$)	0.25	2.69 ($R^2 = 91.95\%$)
TxDOT-TTI_00044 (SH 95)	1.53 ($R^2 = 86.14\%$)	0.27	2.28 ($R^2 = 92.62\%$)
TxDOT-TTI_00026 (SH 358)	0.56 ($R^2 = 28.84\%$)	0.20	6.27 ($R^2 = 100\%$)*
TxDOT-TTI_00069 (SH 44)	0.12 ($R^2 = 43.91\%$)	0.34	0.58 ($R^2 = 100\%$)*

Legend: R_{rc} = rate of reflective cracking per traffic loading ESAL (%cracking/ESAL); R^2 = coefficient of determination; *only two data point after start of cracking, the slope is calculated using two points – therefore, R^2 value = 100%

If the full curve (Slope A) is considered, test section TxDOT-TTI_00024 on SH 95 ($R_{rc} = 1.81$) would be ranked as the poorest section in terms of resistance to reflective cracking, just below TxDOT-TTI_00044, also on SH 95 with $R_{rc} = 1.53$. The best performing test sections, in the top rank, would be US 59 (TxDOT-TTI_00073 and TxDOT-TTI_00001). In general, the rank order of superiority ranking based on Slope A is: TxDOT-TTI_00073 > TxDOT-TTI_00001 > TxDOT-TTI_00069 > TxDOT-TTI_00026 > TxDOT-TTI_00044 > TxDOT-TTI_00024.

Considering Slope B, it is evident in Table 18 that once cracking has initiated, test section TxDOT-TTI_00026 (SH 358) decays at a much faster rate of deterioration than the other test sections. This observation appears to concur with the HMA mix-design volumetrics and the laboratory test results for the Type C mix used on this test section.

Table 1 and Table 2 shows that a coarse-graded (18.75 mm NMAS) Type C mix was used as the overlay on test section TxDOT-TTI_00026 (SH 358) – it has the lowest asphalt-binder content, highest PG grade, and moderate quality limestone aggregates plus RAP. Compared to Slope A (0.56) versus Slope B (6.27), which increased by over 100%, this indicates that mix Type C has a very high propensity for decay once cracking has started – in fact, it has the highest rate of decay in the study matrix, once cracking has started, which has lower tensile strain and *FE*, respectively. Theoretically, its poor performance based on Slope B was not unexpected as this mix (Type C) was also generally ranked at the bottom based on the HMA fracture parameters measured from the monotonic-loading OT test – see the laboratory test results in Table 9 and Table 17.

The Type D₂ mix used on SH 95 (TxDOT-TTI_00024 and TxDOT-TTI_00044) also appears to have a high propensity for rapid deterioration once cracking has started. The slopes, which are greater than 1.00, increased by almost 50% when considering only from the instance cracking started. Overall, the rank order of superiority ranking based on Slope B is: TxDOT-TTI_00001 > TxDOT-TTI_00073 > TxDOT-TTI_00069 > TxDOT-TTI_00044 > TxDOT-TTI_00024 > TxDOT-TTI_00026. Notice that in either ranking scenarios (based on Slope A or Slope B), the test sections on highway US 59, with Type D₁ mix, ranks in the top – which is consistent with the laboratory test results and the mix-design volumetrics discussed previously in Table 9 and Table 17. The overall field performance ranking of the HMA mixes is summarized in Table 19.

Table 19. HMA Mix Field Performance Ranking.

Rank	Rate of reflective cracking per year (%cracking/year)	Slope A, R _{rc} (%) (Full-Curve)	Start of Cracking (MESALs)	Slope B, R _{rc} (%) (From Start of Cracking)
1	TxDOT-TTI_00073 (D ₁)	TxDOT-TTI_00073 (D ₁)	TxDOT-TTI_00073 (D ₁)	TxDOT-TTI_00001 (D ₁)
2	TxDOT-TTI_00069 (D ₃)	TxDOT-TTI_00001 (D ₁)	TxDOT-TTI_00001 (D ₁)	TxDOT-TTI_00073 (D ₁)
3	TxDOT-TTI_00001 (D ₁)	TxDOT-TTI_00069 (D ₃)	TxDOT-TTI_00069 (D ₃)	TxDOT-TTI_00069 (D ₃)
4	TxDOT-TTI_00026 (C)	TxDOT-TTI_00026 (C)	TxDOT-TTI_00044 (D ₂)	TxDOT-TTI_00044 (D ₂)
5	TxDOT-TTI_00044 (D ₂)	TxDOT-TTI_00044 (D ₂)	TxDOT-TTI_00024 (D ₂)	TxDOT-TTI_00024 (D ₂)
6	TxDOT-TTI_00024 (D ₂)	TxDOT-TTI_00024 (D ₂)	TxDOT-TTI_00026 (C)	TxDOT-TTI_00026 (C)

As shown in Table 19, the mix Type D₁ tops based on all the cracking field performance indicators evaluated. These results were not unexpected and are in concurrence with the laboratory asphalt-binder and HMA mix ranking presented previously in Table 17. However, only the parameters “ESALs to start cracking” and *Slope B* ranked the mix Type C at the bottom in the same way as the laboratory tests presented in Table 17 did.

CHAPTER 6

LABORATORY AND FIELD CORRELATIONS

Correlation of the laboratory test data (monotonic loading overlay test, elastic recovery and bending beam rheometer) to field cracking performance was performed considering the following six methodological approaches were considered:

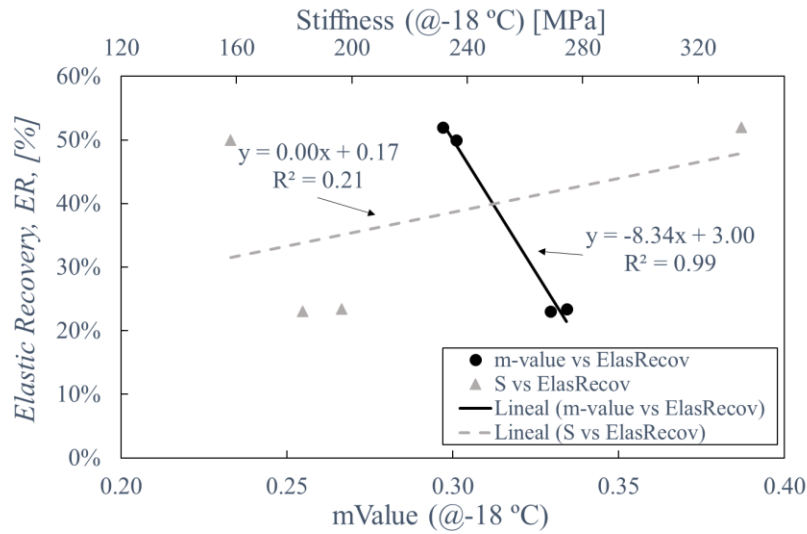
- a) Percentage reflection cracking (%cracking) as a function of time at 41.77 months (3.48 years) determined from Figure 11. Note that based on Figure 11, 41.77 months is longest service life endured by the test sections on SH 95 and hence, it (41.77 months) was used as the reference datum to ensure similar age comparisons.
- b) Rate (slope) of reflective cracking per year (i.e., %cracking/year) determined from Figure 11.
- c) Percentage reflection cracking (%cracking) as a function of traffic loading at 0.24 million ESALs determined from Figure 12. Note that based on Figure 12, 0.24 million ESALs is the maximum traffic loading endured by the test sections on SH 358 as at the time of writing this document and hence, it (0.24 million) was used as the reference datum to ensure similar traffic loading comparisons.
- d) The number of traffic loading ESALs to start of cracking on each highway test sections, representing the crack initiation phase – determined from Fig. 6.
- e) Slope A of the full curves in Figure 12, representing the crack initiation and propagation phases, respectively.
- f) Slope B of the curves from the instance cracking started (Figure 12), representing the crack propagation phase.

Table 20. Field Cracking Performance Parameters

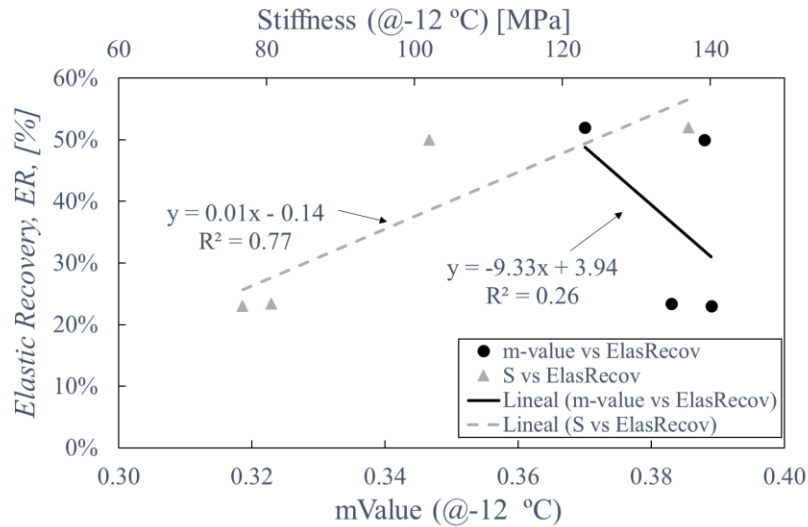
Section ID (Hwy)	Approach					
	A (%RC)	B (%RC/Year)	C (%RC)	D MESALs	E (%RC/MESAL)	F (%RC/MESAL)
TxDOT-TTL_00001 (US 59)	2.90%	1.80%	0.00%	2.75	0.02	0.04
TxDOT-TTL_00073 (US 59)	0.00%	0.00%	0.00%	N/A	0.00	0.00
TxDOT-TTL_00024 (SH 95)	92.86%	31.05%	0.00%	0.25	1.81	2.69
TxDOT-TTL_00044 (SH 95)	85.71%	28.60%	0.00%	0.27	1.53	2.28
TxDOT-TTL_00026 (SH 358)	0.00%	1.82%	25.50%	0.20	0.56	6.27
TxDOT-TTL_00069 (SH 44)	4.86%	1.50%	0.00%	0.34	0.12	0.58

6.1. Correlations of Asphalt Binder Laboratory Test Results

In this section, the measured asphalt-binder low temperatures properties, namely *ER*, *S*, and *m-value* were correlated. The comparisons of the ER and BBR tests are presented in Figure 13.



(a) ER versus BBR at -18 °C



(b) ER versus BBR at -12 °C

Figure 13. Asphalt-Binder Low Temperature Correlations.

From Figure 13 (a), the *ER* of the asphalt-binders appear to have a good statistical correlation with the *m-value* obtained with the BBR conducted at -18 °C, with R^2 values exceeding 60%. By contrast, however, the *ER* exhibited the lowest statistical correlation with stiffness at this temperature, with the R^2 values below 30%. Using the BBR conducted at -12 °C, the *ER* shows good statistical correlation to stiffness, with the R^2 value exceeding 70%. However, the *m-value* ($R^2 = 26\%$) appears to have a comparatively low statistical correlation.

6.2. Correlations of Laboratory Asphalt Binder to HMA Fracture Properties

Based on numerous curve fitting trials of the laboratory test data, a logarithmic trendline was selected as the best regression fit, with the generalized model illustrated in Eq. 10.

$$y = \alpha \ln(x) + \beta \tag{Eq. 10}$$

Where, parameter y is the laboratory measured data from the M-OT test representing the HMA fracture parameters (namely peak load, tensile strength, tensile strain, tensile modulus, FE , and FE Index), x is the low temperature property (namely ER , S , m -value) representing the asphalt-binder properties, and α and β are regression coefficients.

6.2.1. Asphalt-Binder Elastic Recovery (ER) versus HMA Fracture (M-OT) Properties.

Using the proposed fitting model the measured asphalt-binder elastic recovery (ER) presented in Table 5 and the HMA fracture properties obtained from the monotonic loading overlay test (OT) presented in Table 9 were correlated.

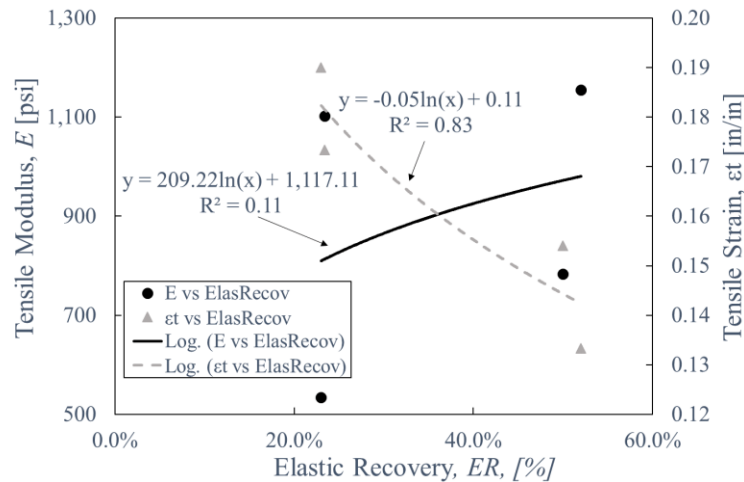


Figure 14. Asphalt-Binder Elastic Recovery - Tensile Modulus and Tensile Strain Correlation.

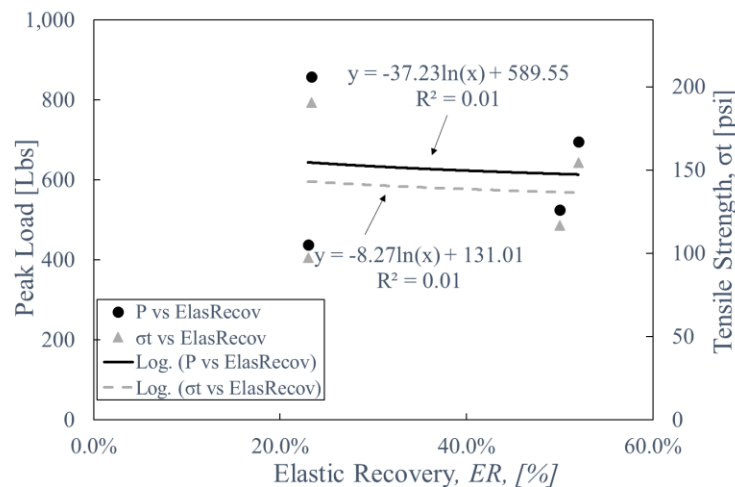


Figure 15. Asphalt-Binder Elastic Recovery – Peak Load and Tensile Strength Correlation.

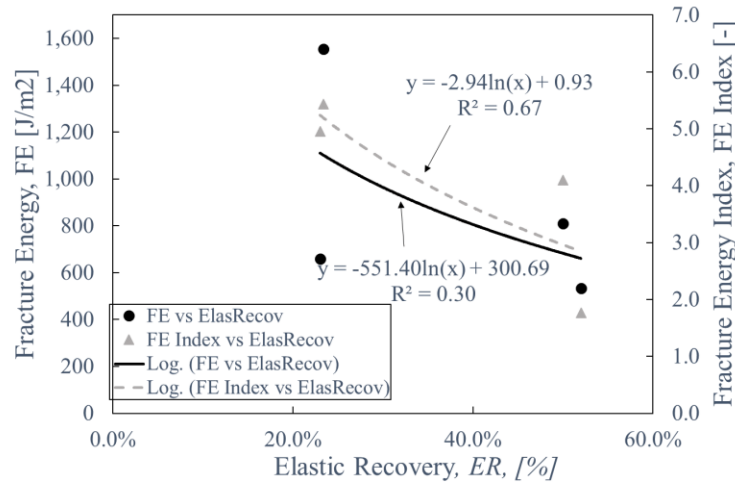
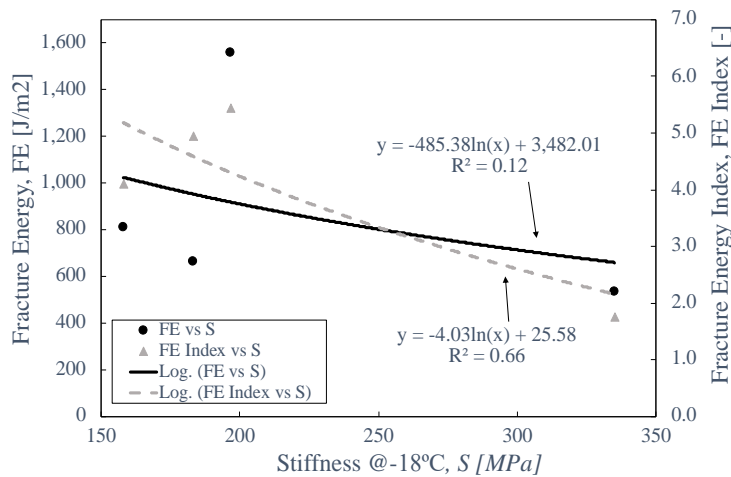


Figure 16. Asphalt-Binder Elastic Recovery – FE and FEI Correlation.

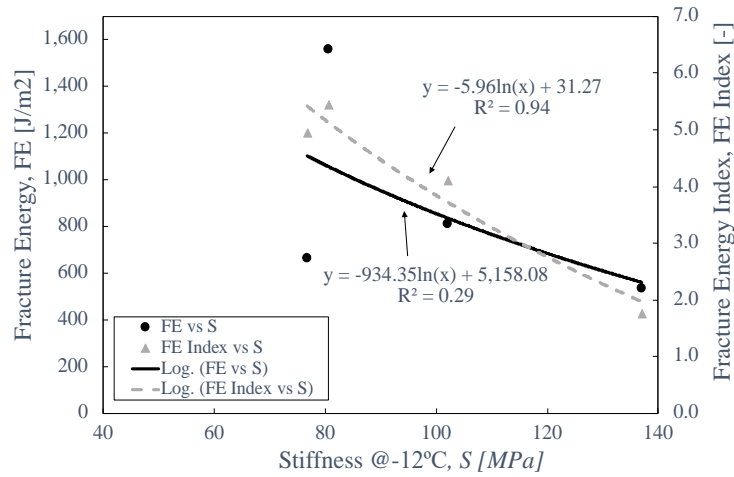
6.2.2. Asphalt-Binder Bending Beam Rheometer (BBR) versus HMA Fracture (M-OT) Properties.

Using the proposed fitting model (Eq 10.) the parameters obtained from the Bending Beam Rheometer conducted at -12°C and -18°C presented in Table 7 and the HMA fracture properties obtained from the monotonic loading overlay test (OT) presented in Table 9 were correlated.

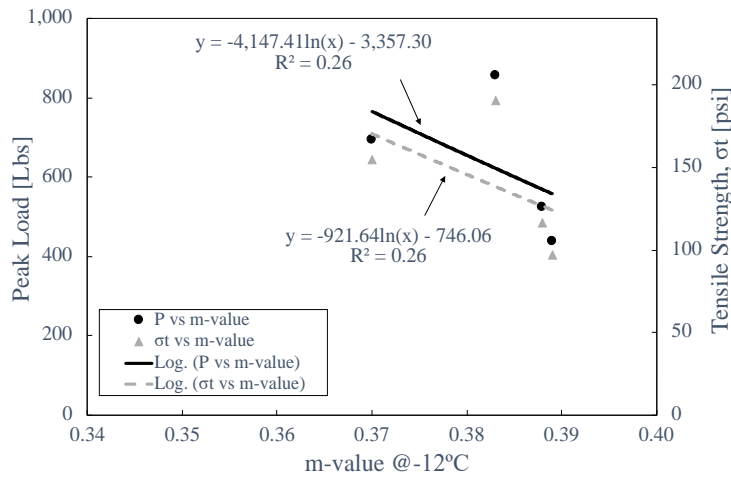
Figure 17 exemplifies some randomly selected and plotted trend-lines between the asphalt-binder low-temperature properties obtained from the BBR and the HMA fracture properties obtained from the M-OT test.



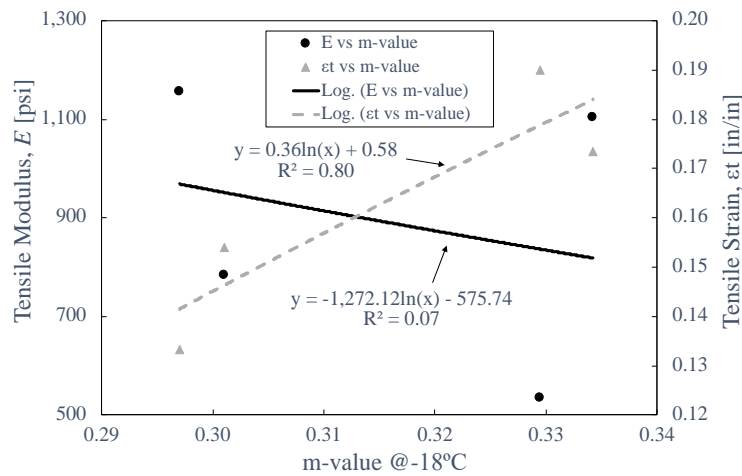
(a) FE and FE index versus S at -18°C



(b) FE and FE index versus S at -12 °C



(c) P and σ_t versus m-value at -12 °C



(d) E and ϵ_t versus m-value at -18 °C

Figure 17. Asphalt-Binder HMA Correlations.

Table 21 summarizes the regression coefficients (α , β) and the R^2 values computed using logarithmic models for the evaluated correlations (ER and BBR vs M-OT). The R^2 values obtained in the regression analysis represent a measure/indicator of the statistical strength of the correlation between the laboratory test data. For easy comparative analysis, the asphalt-binder low temperature properties were arranged in a descending order of statistical superiority based on the magnitude of R^2 value.

Table 21. Regression Coefficients α , β , and R^2 for Asphalt Binder to HMA Fracture Properties.

HMA Fracture Parameter (M-OT) (y)	Asphalt-Binder Low Temperature Parameter (x)	α	β	R^2
<i>Tensile strain (ϵ_t)</i>	Stiffness @-12°C	-0.09	0.57	0.95
	Elastic Recovery	-0.05	0.11	0.83
	m-value @-18°C	0.36	0.58	0.80
	m-value @-12°C	0.83	0.96	0.61
	Stiffness @-18°C	-0.05	0.42	0.43
<i>Tensile modulus (E)</i>	m-value @-12°C	-10058.07	-8774.29	0.64
	Stiffness @-18°C	585.95	-2236.18	0.44
	Stiffness @-12°C	616.40	-1922.41	0.32
	Elastic Recovery	209.22	1117.11	0.11
	m-value @-18°C	-1272.12	-575.74	0.07
<i>Peak load (P)</i>	m-value @-12°C	-4147.41	-3357.30	0.26
	Stiffness @-18°C	222.53	-559.38	0.15
	m-value @-18°C	523.49	1234.01	0.03
	Stiffness @-12°C	95.06	194.98	0.02
	Elastic Recovery	-37.23	589.55	0.01
<i>Tensile strength (σ_t)</i>	m-value @-12°C	-921.64	-746.06	0.26
	Stiffness @-18°C	49.45	-124.31	0.15
	m-value @-18°C	116.33	274.22	0.03
	Stiffness @-12°C	21.12	43.33	0.02
	Elastic Recovery	-8.27	131.01	0.01
<i>Fracture energy (FE)</i>	m-value @-18°C	4862.12	6505.88	0.42
	Elastic Recovery	-551.40	300.69	0.30
	Stiffness @-12°C	-934.35	5158.08	0.29
	Stiffness @-18°C	-485.38	3482.01	0.12
	m-value @-12°C	4840.19	5541.77	0.06
<i>Fracture Energy Index (FE Index)</i>	Stiffness @-12°C	-5.96	31.27	0.94
	m-value @-18°C	23.04	30.68	0.74
	m-value @-12°C	58.84	60.62	0.69
	Elastic Recovery	-2.94	0.93	0.67
	Stiffness @-18°C	-4.03	25.58	0.66

FE Index shows a good correlation ($R^2 > 60\%$) with all the evaluated asphalt-binder low temperature properties. This indicates that *FE Index* could be predicted and estimated from the evaluated asphalt-binder low temperature parameters using the logarithmic model to an accuracy or reliability/certainty exceeding 60%. *Stiffness (S)* from the BBR conducted at -12 °C appears to be a good predictor of the HMA *FE Index* – with a R^2 value as high as 94%, i.e., reliability/certainty of about 94%.

Tensile strain (ϵ_t) also exhibited good correlation with the ER test (ductility), *stiffness*, and *m-value* measured at -12°C, and the *m-value* from the BBR conducted at -18°C. Again

stiffness (S) from the BBR conducted at $-12\text{ }^{\circ}\text{C}$ appears to be a good predictor of the HMA fracture parameter ($R^2 = 95\%$). In the cases of *stiffness* and ER , these two variables are inversely related, and directly proportional in the case of *m-value*. *Tensile modulus* (E) only exhibited a good correlation to the *m-value* from the BBR test conducted at $-12\text{ }^{\circ}\text{C}$. By contrast, all the asphalt-binder low temperature properties evaluated exhibited comparatively low statistical correlation with the R^2 values below 50% (i.e., less than 50% accuracy/certainty) to predict *peak load* (P), *tensile strength* (σ_t), and *fracture energy* (FE).

In general, *tensile strain* (ϵ_t) and *FE Index* yielded the highest statistical correlation to the asphalt-binder low temperature properties from the ER and BBR tests, with R^2 values exceeding 60% (predictive certainty). The *stiffness* obtained from the BBR test at $-12\text{ }^{\circ}\text{C}$ appears to be a good predictor of the *tensile strain* and *FE Index*, with R^2 values exceeding 90%. It is also worthwhile to note that there was no clear trend between the low temperature asphalt-binder properties with the following HMA fracture parameters: *peak load* (P), *tensile strength* (σ_t), and FE – all the R^2 values were below 50%.

6.3. Correlations of Laboratory Asphalt Binder to Field Performance

As mentioned before, Correlation of the asphalt-binder laboratory test data to field cracking performance was performed based on considering a similar reference datum for all the highway sections using $R^2 \geq 60\%$ as an indicative measure of good statistical correlation and predictive certainty. The six methodological approaches proposed in Table 20 were correlated with the asphalt binder low temperature properties obtained from the BBR and ER using simple linear regression model illustrated in Eq. 11:

$$y = ax + b \quad (\text{Eq. 11})$$

Where, parameter y is the field data representing the six methodological approaches adopted (namely %cracking at 41.77 months, %cracking at 0.24 MESALs, traffic ESALs at start of cracking, and the slopes [%cracking/MESALs]), x is the low-temperature property (namely ER , S , *m-value*) representing the asphalt-binder properties, and a (slope) and b (intercept) are regression coefficients.

6.3.1. Asphalt-Binder Elastic Recovery (ER) versus Field Cracking Performance

Using the proposed fitting model (Eq 11.) the measured asphalt-binder elastic recovery (ER) presented in Table 5 and the field cracking performance presented in Table 20 were correlated.

Figure 18 and Figure 19 exemplifies some randomly selected and plotted trend-lines between the asphalt-binder low-temperature properties obtained from the ER and the six methodological approaches proposed for field performance.

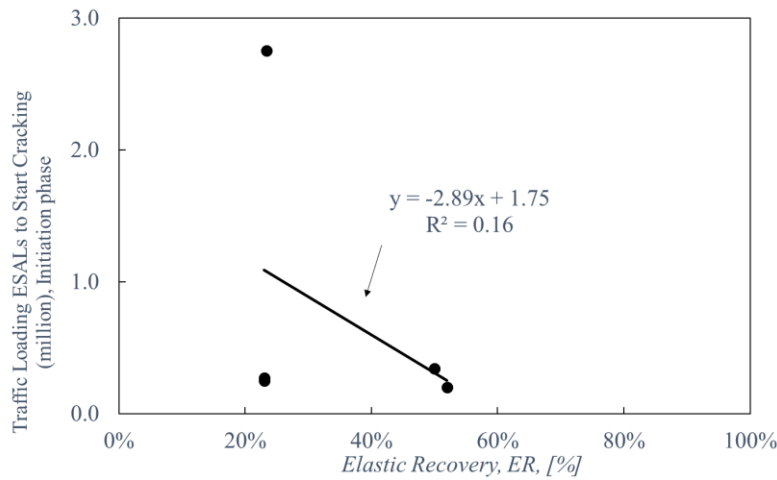


Figure 18. ER – Approach D Correlation.

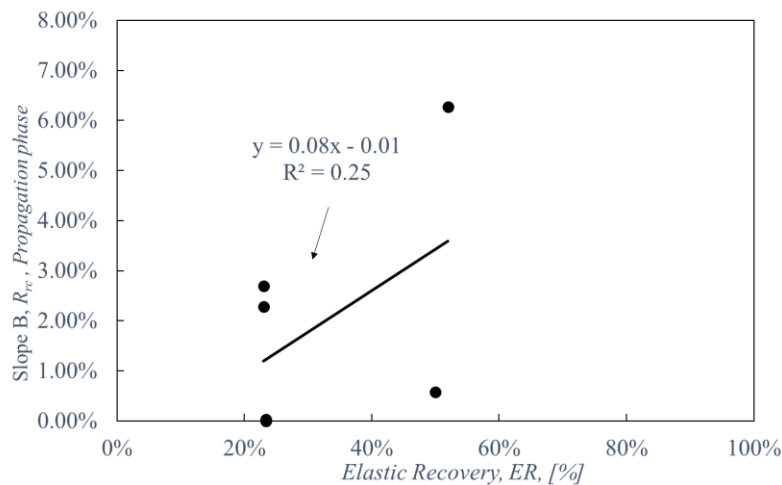
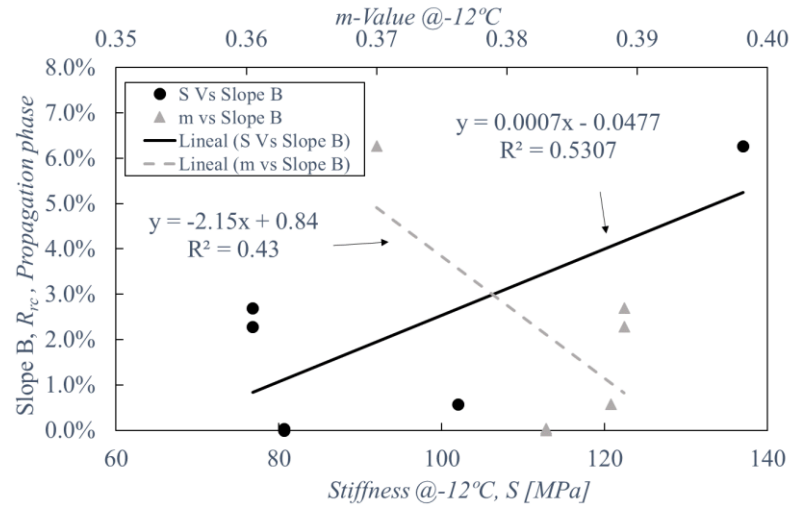


Figure 19. ER – Approach F Correlation.

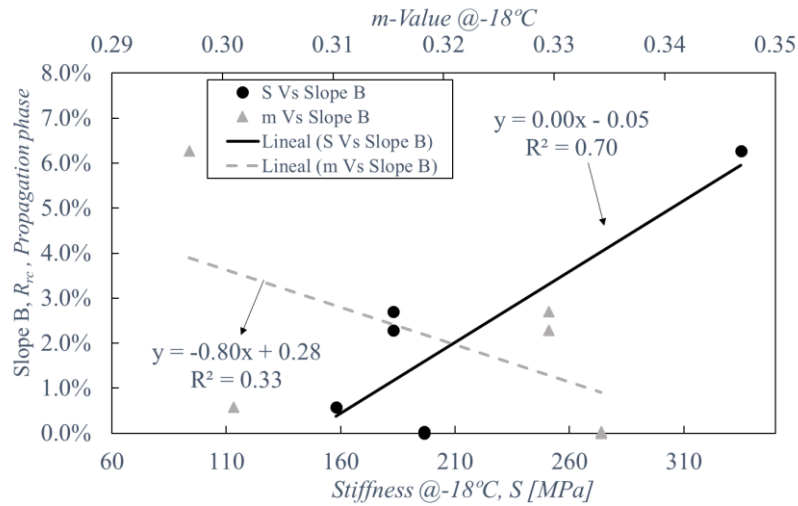
6.3.2. Asphalt-Binder Bending Beam Rheometer (BBR) versus Field Cracking Performance

Using the proposed fitting model (Eq 11.) the parameters obtained from the Bending Beam Rheometer conducted at -12°C and -18°C presented in Table 7 and the field cracking performance presented in Table 20 were correlated.

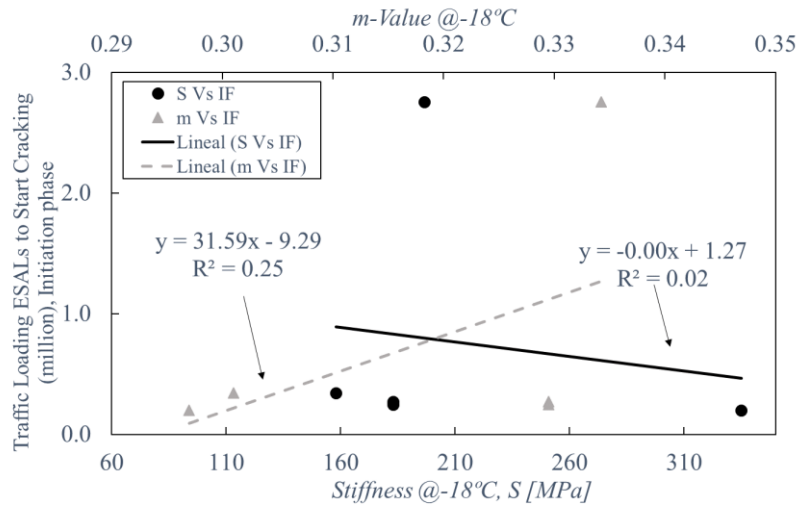
Figure 20 exemplifies some randomly selected and plotted trend-lines between the asphalt-binder low-temperature properties obtained from the BBR and the six methodological approaches proposed for field performance.



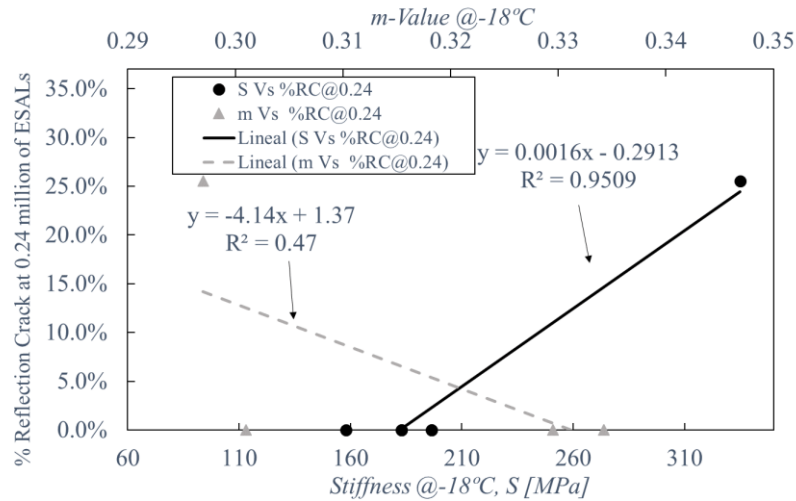
(a) Slope B versus S and m -value at -12 °C



(b) Slope B versus S and m -value at -18 °C



(c) MESAL at Crack Start versus S and m -value at -18 °C



(d) %cracking at 0.24MESAL versus S and m -value at -18°C

Figure 20. BBR-Field Reflective Cracking Correlation Plots.

Similar to Table 21, Table 22 summarizes all the regression coefficients (a, b) and the R^2 values based on the proposed fitting trend line. The asphalt-binder low-temperature properties were arranged in a descending order of statistical superiority based on the magnitude of R^2 value to easily evaluate the ability of each laboratory parameter to predict the field cracking performance of the HMA mixes. From Table 22, only the reflective cracking as a function of traffic loading (approach c) and *Slope B* appears to have good correlation with the field cracking performance. Using the percentage of cracking at 0.24 million ESALs as the field performance approach, the parameters S and m -value from the BBR conducted at -12°C and the stiffness measured with the BBR test at -18°C exhibit a good ability to predict reflective cracking behavior, with R^2 values exceeding 80%. With an R^2 value of 70%, the *stiffness* measured at -18°C exhibit great potential to predict the field cracking behavior base on approach f – *Slope B* (%cracking/MESAL) representing the crack propagation phase.

Table 22. Regression Coefficients m , b and R^2 in Equation 11.

#	Approach (y)	Asphalt-Binder Low Temperature Parameter (x)	a	b	R^2
a	Reflection cracking as a function of time (%Crack at 41.77 months)	m -value @ -12°C	36.89	-13.84	0.35
		Stiffness @ -12°C	-0.01	1.20	0.26
		Elastic Recovery	-1.58	0.82	0.25
		m -value @ -18°C	10.02	-2.91	0.14
		Stiffness @ -18°C	-0.00	0.81	0.12
b	Rate of reflective cracking per year (%cracking/year)	m -value @ -12°C	11.34	-4.24	0.31
		Elastic Recovery	-0.50	0.27	0.24
		Stiffness @ -12°C	-0.003	0.38	0.23
		m -value @ -18°C	3.14	-0.90	0.13
		Stiffness @ -18°C	-0.0007	0.253	0.09
c	Reflection cracking as a function of traffic loading (%cracking at 0.24 million ESALs)	Stiffness @ -18°C	0.0016	-0.2913	0.95
		m -value @ -12°C	-13.23	5.12	0.85
		Stiffness @ -12°C	0.004	-0.327	0.84
		m -value @ -18°C	-4.14	1.37	0.47
		Elastic Recovery	0.48	-0.11	0.44

#	Approach (y)	Asphalt-Binder Low Temperature Parameter (x)	a	b	R ²
d	Initiation phase (traffic ESALs to start of cracking)	<i>m-value</i> @-18°C	31.59	-9.29	0.25
		<i>Elastic Recovery</i>	-2.89	1.75	0.16
		<i>Stiffness</i> @-12°C	-0.01	2.06	0.10
		<i>Stiffness</i> @-18°C	-0.00	1.27	0.02
		<i>m-value</i> @-12°C	-3.10	1.95	0.00
e	Initiation and Propagation phases (<i>Slope A</i>)	<i>m-value</i> @-12°C	0.41	-0.15	0.14
		<i>Elastic Recovery</i>	-0.02	0.01	0.10
		<i>Stiffness</i> @-12°C	0.00	0.02	0.07
		<i>m-value</i> @-18°C	0.09	0.02	0.04
		<i>Stiffness</i> @-18°C	0.00	0.01	0.01
f	Propagation phase (<i>Slope B</i>)	<i>Stiffness</i> @-18°C	0.0003	-0.05	0.70
		<i>Stiffness</i> @-12°C	0.0007	-0.05	0.53
		<i>m-value</i> @-12°C	-2.15	0.84	0.43
		<i>m-value</i> @-18°C	-0.80	0.28	0.33
		<i>Elastic Recovery</i>	0.08	-0.01	0.25

Legend: α and β are logarithmic regression coefficients; R^2 = coefficient of determination

The *ER* and the *m-value* from the BBR test conducted at -18 °C shows comparatively low correlation to predict field reflective cracking performance in all the six approaches with the R^2 values below 50%. As evident in Table 22, the best statistical correlations were associated the reflective cracking as a function of traffic loading (Approach c) and the *stiffness* measured with the BBR at -18°C, with R^2 values of 95%, i.e., 95% accuracy and predictive certainty. The lowest statistical correlation was generally associated with *Slope A*, with R^2 values below 14% for all the asphalt-binder low temperature properties, i.e., predictive certainty and accuracy lower than 14%.

For the materials and highway sections evaluated in this study, most of the asphalt-binder low temperature properties exhibited statistical correlation with field HMA reflective cracking, with prediction certainty/accuracy lower than 50% (based on the R^2 values). It appears that only when reflection cracking as a function of traffic loading is used as the field performance indicator, do the asphalt-binder low temperature properties (*stiffness* at -12°C and -18°C, and *m-value* at -12°C) present high potential accuracy (> 60%) and certainty to predict field cracking performance. Considering that different inbuilt standard model fit-lines in MS Excel (such as logarithmic, power, exponent, etc.) were tried, it is apparent that probably more advanced statistical correlations such as logistic models need to be explored in future studies.

6.4. Fracture (M-OT) Properties versus Field Performance

Based on numerous curve fitting trials of the laboratory to field data using the above methodological approaches, a logarithmic trendline was selected as the best regression fit, with the generalized logarithmic model illustrated in Eq. 12:

$$y = \alpha \ln(x) + \beta \quad (\text{Eq. 12})$$

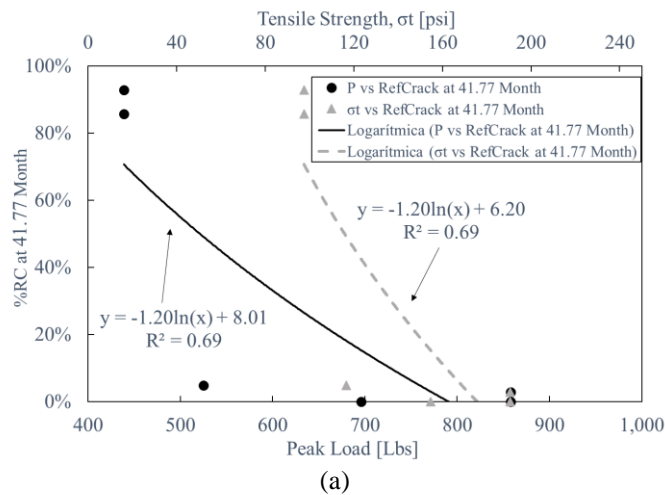
In Eq. 12, parameter y is the field performance representing reflective cracking (namely %cracking, rate of cracking (slope), traffic loading ESALs, etc.), x is the laboratory measured data from the monotonic-loading OT test representing the HMA fracture parameters (namely

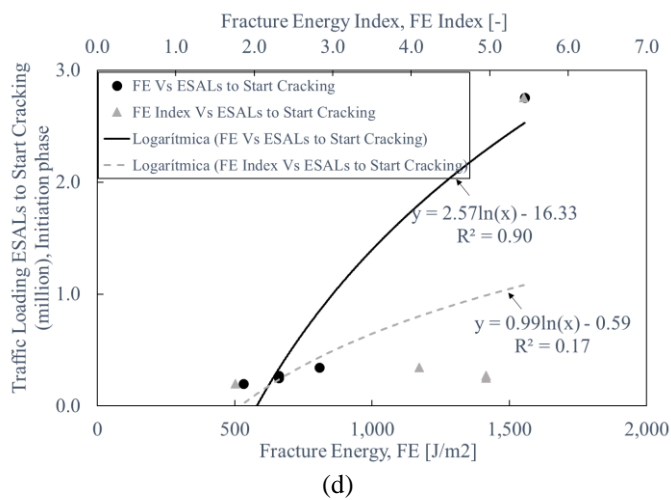
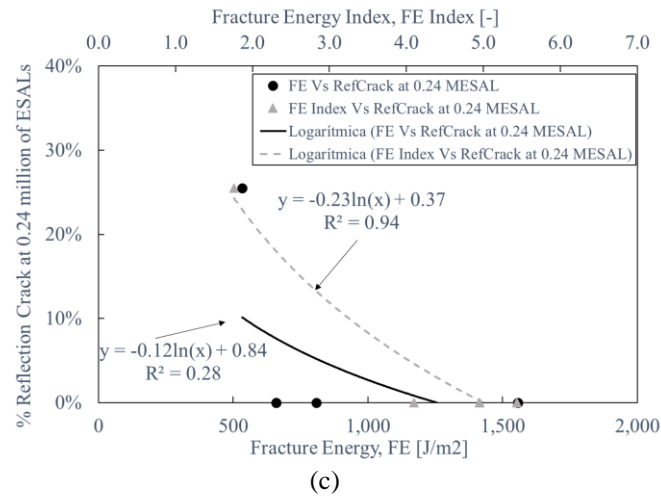
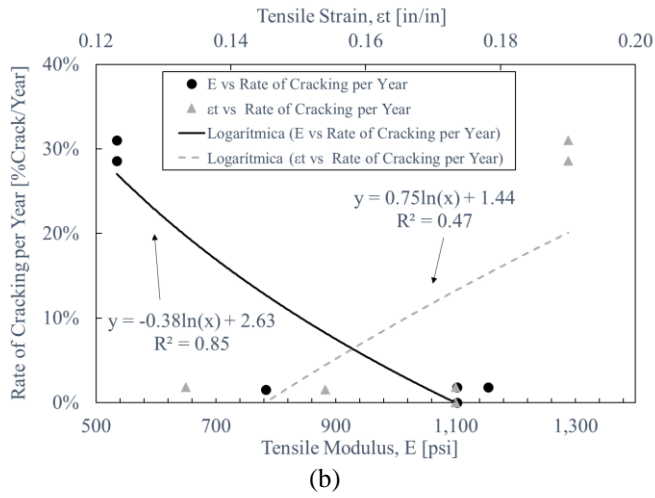
peak load, tensile strength, tensile strain, tensile modulus, *FE*, and *FE Index*), and α and β are regression coefficients defining the logarithmic relationship between laboratory and field performance data.

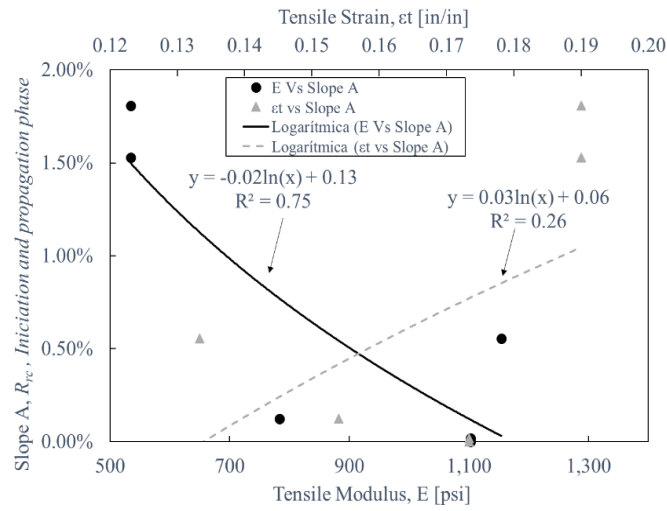
Figure 21 exemplifies some randomly selected and plotted logarithmic relationships for each of the six methodological approaches, with field performance data on the vertical Y-axis and the laboratory measured HMA fracture parameters on the horizontal X-axis. The regression equation (i.e., logarithmic fit function in Eq. 12) and coefficients of determination (R^2) are also indicated on each graph.

Table 23 summarizes the regression coefficients (α , β) and the R^2 values using logarithmic trend lines for each of the six methodological approaches discussed above. The R^2 values obtained in the regression analysis allows to evaluate the ability of each HMA fracture parameter to predict the field performance of the HMA mix. In other words, it is a statistical measure/indicator of the statistical strength of the correlation between the laboratory and field performance data – quantifying how statistically accurate the respective HMA fracture parameter is able to correlate and predictive the indicated field performance data, i.e., reflective cracking. For easy comparative analysis, the HMA fracture parameters in each methodological approach, in

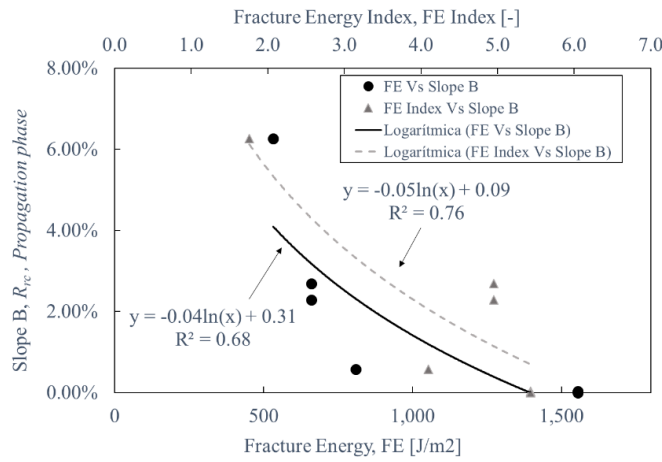
Table 23, were arranged in a descending order of statistical superiority based on the magnitude of R^2 value.







(e)



(f)

Figure 21. Relationship between Monotonic OT parameters and field performance in the (a) Reflection cracking as a function of time (b) Rate of reflective cracking per year (c) Reflection cracking as a function of traffic loading (d) Initiation phase (e) Initiation and propagation phase (f) Propagation phase

Table 23. Regression Coefficients α , β and R^2 in Equation 12.

#	Approach (y)	HMA Fracture Parameter (x)	α	β	R^2
a	Reflection cracking as a function of time (%Crack at 41.77 months)	Tensile modulus (E)	-1.16	8.12	0.87
		Peak load (P)	-1.20	8.01	0.69
		Tensile strength (σ_t)	-1.20	6.20	0.69
		Tensile strain (ϵ_t)	2.35	4.51	0.51
		Fracture energy (FE)	-0.46	3.43	0.22
		Fracture Energy Index ($FE Index$)	0.33	-0.17	0.10
b	Rate of reflective cracking per year (%cracking/year)	Tensile modulus (E)	-0.38	2.63	0.85
		Peak load (P)	-0.39	2.61	0.68
		Tensile strength (σ_t)	-0.39	2.02	0.68
		Tensile strain (ϵ_t)	0.75	1.44	0.47
		Fracture energy (FE)	-0.16	1.18	0.24
		Fracture Energy Index ($FE Index$)	0.10	-0.03	0.08
c		Fracture Energy Index ($FE Index$)	-0.23	0.37	0.94

#	Approach (y)	HMA Fracture Parameter (x)	α	β	R^2
	Reflection cracking as a function of traffic loading (%cracking at 0.24 million ESALs)	Tensile strain (ϵ_t)	-0.63	-1.08	0.68
		Fracture energy (FE)	-0.12	0.84	0.28
		Tensile modulus (E)	0.13	-0.83	0.21
		Peak load (P)	0.07	-0.39	0.04
		Tensile strength (σ_t)	0.07	-0.29	0.04
d	Initiation phase (traffic ESALs to start of cracking)	Fracture energy (FE)	2.57	-16.33	0.90
		Peak load (P)	2.85	-13.04	0.57
		Tensile strength (σ_t)	2.85	-13.04	0.57
		Tensile modulus (E)	1.52	-9.32	0.26
		Fracture Energy Index ($FE Index$)	0.99	-0.59	0.17
		Tensile strain (ϵ_t)	1.14	2.81	0.02
e	Initiation and Propagation phases (Slope A)	Tensile modulus (E)	-0.02	0.13	0.75
		Peak load (P)	-0.02	0.14	0.69
		Tensile strength (σ_t)	-0.02	0.11	0.69
		Fracture energy (FE)	-0.01	0.08	0.43
		Tensile strain (ϵ_t)	0.03	0.06	0.26
		Fracture Energy Index ($FE Index$)	0.00	0.01	0.00
f	Propagation phase (Slope B)	Fracture Energy Index ($FE Index$)	-0.05	0.09	0.76
		Fracture Energy (FE)	-0.04	0.31	0.68
		Tensile Strain (ϵ_t)	-0.09	-0.15	0.28
		Peak Load (P)	-0.02	0.14	0.06
		Tensile Strength (σ_t)	-0.02	0.11	0.06
		Tensile Modulus (E)	-0.00	0.03	0.00

Legend: α and β are logarithmic regression coefficients; R^2 = coefficient of determination

For interpretation of the results in

Table 23, a high R^2 value means good statistical correlation with good predictive potential (reflective cracking) for the HMA fracture parameter – and vice versa for lower R^2 values. Conversely, tensile modulus (E_t), peak load (P), and tensile strength (σ_t) yielded the highest correlation, with R^2 values exceeding 60%, using the percentage of reflective cracking as a function of time (at 41.77 months or 3.48 years) and rate of reflective cracking per year (i.e., %cracking/year), both approaches taking into account only time regardless of the differences in traffic loading. By contrast, the FE and $FE Index$ exhibited the poorest statistical correlation with the R^2 values below 30% as a function of time. However, if the traffic loading is considered, using the percentage reflection cracking at a fixed traffic loading (0.24 million ESALs in approach [c]), $FE Index$ appears to be a good indicator and predictor of the reflective cracking field performance – with a R^2 value as high as 94%.

When considering the initiation phase (approach [d]) of the cracking phenomenon modeled with the number of traffic loading ESALs to start cracking, FE tops the rank with a with a R^2 value of 90%, whilst all the other HMA fracture parameters registered R^2 values below 60%. For the crack propagation phase, defined by Slope B (approach [f]), both the FE and $FE Index$, with R^2 values exceeding 60%, appear to have good statistical correlations with the field performance data. The rest of the HMA fracture parameters, all have R^2 values less than 30% in approach (f) – crack propagation. For the complete analysis of the reflective cracking phenomenon using the Slope A (approach [e]), taking into account both the initiation and propagation phases, tensile modulus (E_t), peak load (P), and tensile strength (σ_t) yielded the best correlation with R^2 values exceeding 60%.

Overall, the best statistical correlation-ship with the highest R^2 values, at or above 90%, was registered for the *FE* and *FE Index* parameters when traffic loading is taken into account (approach [c] and [d]). In general, the R^2 values obtained in this study are comparable and, in some instances, better than those reported in the literature. For instance, Oshone et al. [76] reported R^2 values ranging from low 5% to as high as 75% - whilst the R^2 range in Table 9 is a poor 1% to an astounding 94%.

6.5. Summary

In this chapter, the laboratory predictions and field correlations were performed using six methodological approaches. The key outcomes from the chapter are as follows:

- The measured asphalt-binder low temperatures properties, namely *ER*, *S*, and *m-value* were correlated.
- The correlation between laboratory asphalt binder and HMA fracture properties were performed.
- The asphalt binder low temperature properties from the BBR and ER were correlated to the field performance using the six methodological approaches.
- The monotonic loading Overlay Test fracture parameters were also correlated to the proposed field performance approaches.

CHAPTER 7

SUMMARY, CONCLUSIONS AND RECOMMENDATIONS

7.1. Synthesis and Discussion of the Results and Findings

The ability of the monotonic-loading OT test and the HMA fracture parameters to differentiate the mixes were evaluated using ANOVA and Tukey's HSD statistical methods. The rank order of superiority for the HMA fracture parameters to statistically differentiate mixes was found to be as follows: P_{max} , σ_t , and $FE > E_t$ and $FE Index > \epsilon_t$. Tensile strain does not appear to be a good HMA fracture parameter to statistically differentiate the HMA mixes – it failed to differentiate the mixes and, as was shown in Table 16 it ranked all the mixes into one statistical group. Peak Load, Tensile Strength and Fracture Energy appears to have a good ability to statistically differentiate between mixes (3 Groups), this is based on the fact that these are the parameters that have the lowest variability as can be seen in Figure 9. A high proximity of the average values of the *Elastic Recovery* (ER) and *m-value* (BBR) and *tensile strain* (M-OT) was obtained, suggesting a possible shortcoming in the ability of this parameter to statistically differentiate and statistically discriminate among the tested asphalt-binders, this hypothesis were evaluated for *tensile strain* during the ANOVA and Tukey's HSD analysis.

As theoretically expected of monotonic-loading crack tests, Table 9 and Figure 9 showed that the HMA fracture parameters obtained from the monotonic-loading OT test are fairly repeatable with low values (COV < 30%) – thus, substantiating the consistency and quality of the output data from the test. The *Peak Load* and *Tensile Strength* obtained from the M-OT appears to be the parameters with the best consistency and statistical credibility/confidence based on the variability with COV values lower than 10%. The *Fracture Energy Index* and *Tensile Modulus* appear to be the most variable HMA fracture parameters, with the highest COV values averaging 20.0% and 18.0%, respectively. In terms of statistical credibility and confidence, the HMA fracture parameters would be ranked as follows: P_{max} and σ_t , > $FE > \epsilon_t$ > $FE Index > E_t$. From the Asphalt binder test results, it is noted that the ER test yielded a good statistical credibility in the ER tests with COV values averaging 2.50%. For the BBR only one specimen replicate was tested per asphalt-binder, therefore, any parameter of variance cannot be calculated.

The *stiffness* and *m-value* obtained from the BBR test were compared with the *ER* measured from the ductilometer test to search for a relationship among the three asphalt-binder low temperature properties. The *ER* showed good statistical correlation to stiffness measured with the BBR test conducted at -12°C ($R^2 = 77\%$) and with the *m-value* performed at -18°C ($R^2 = 99\%$), i.e., predictive certainty and accuracy greater than 60%.

The ability of the asphalt-binder low-temperature properties to predict the HMA fracture properties from the M-OT test were also evaluated. The comparison of the ER and BBR test results suggest that tensile strain (ϵ_t) and *FE Index* have a good correlation with the asphalt-binder low temperature properties from the ER and BBR tests. This means that these can be good predictors of ϵ_t and *FE Index*, with R^2 values exceeding 60%, i.e., predictive certainty and accuracy greater than 60%. However, all of the evaluated asphalt-binder parameters

exhibited predictive certainty/accuracy less than 50% with the following HMA fracture properties: *peak load*, *tensile strain*, and *FE* – the R^2 values were all below 50%. By contrast, the *m-value* obtained from BBR at -12°C seems to be a good predictor of the tensile modulus, with $R^2 = 64\%$.

Correlation of the laboratory test predictions to field performance of the in-service highways sections was comparatively evaluated and analyzed taking into account both time and traffic loading using six methodological approaches. Most of the asphalt-binder low temperature properties used in this study exhibited statistical correlation and prediction certainty/accuracy lower than 50% to reflective cracking field performance. However, only using reflective cracking at 0.24 MESALs as the field performance indicator did the low-temperature asphalt-binder properties parameters exhibit high potential and certainty/accuracy ($> 60\%$) as the HMA cracking performance predictors. In line with these results, Nsengiyumva [59] found that evaluating the cracking behavior in HMA mixes by only considering low-temperature properties of asphalt-binder as the PG system [18] may therefore not be an adequate practice. The approach is not exhaustive and does not take into account the aggregate matrix in the HMA mix. This could partially explain the low statistical correlations observed for most of the asphalt-binder low temperature properties evaluated in this document.

Correlation of the HMA fracture properties (from M-OT) to field performance of the in-service highways sections was also comparatively evaluated and analyzed taking into account both time and traffic loading. If the ability to differentiate the mixes (statistical grouping ≥ 2), data variability ($COV \leq 30\%$), and statistical correlation ($R^2 \geq 60\%$) with field performance data are considered, the most promising HMA fracture parameters to correlate and predict reflective cracking performance in the field (for the proposed approaches) would be as follows:

- a) Percentage cracking as a function of time = P_{max} , σ_t , and E_t
- b) Rate of cracking per year = P_{max} , σ_t , and E_t
- c) Percentage cracking as a function of traffic loading and time = *FE Index*.
- d) Traffic loading ESALs to start of cracking (crack initiation) = *FE*
- e) Complete cracking phenomenon = E_t , P_{max} and σ_t
- f) Rate of cracking after start of cracking (crack propagation) = *FE* and *FE Index*.

In consideration of the above analysis and the results exemplified in Figure 12 as well as the fact only the HMA mixes and test sections on highways SH 358 and SH 95 had exceeded 25% reflective cracking at the time of writing this paper, the following thresholds are proposed as the tentative pass-fail screening criteria for the monotonic loading OT test: $P_{max} \geq 500$ lb, $100 \geq \sigma_t \leq 200$ psi, $E_t \geq 700$ psi, $FE \geq 700$ J/m², and *FE Index* ≥ 5.00 . Note that these proposed criteria, solely based on the HMA mixes and highway sections evaluated in this study, are tentative and are therefore, not exhaustive.

7.2. Conclusions

This study correlated and preliminarily validated the laboratory asphalt binder low temperatures properties and monotonic-loading OT test to field crack performance of in-

service highway sections. Various asphalt-binder low temperature properties measured from the BBR and ER tests and HMA fracture parameters obtained from the monotonic-loading OT test were evaluated in terms of their ability to statistically differentiate the mixes, data variability, and statistical correlation with field performance.

The primary idea was to evaluate/select the most promising asphalt-binder low temperature properties and HMA fracture parameters to correlate and predict reflective cracking performance of mixes in the field. The Texas DSS was used as the primary data source for both laboratory (four HMA mixes) and field (six in-service highway sections) data used in the study. Based on the results and findings presented herein, the following conclusions and recommendations were drawn:

- The monotonic-loading OT test is a fairly repeatable test with the potential to statistically differentiate and screen HMA mixes relative to field performance. The data quality from the monotonic-loading OT test is of acceptable statistical consistency and reliability, with COV values less than 30%. Similarly, the ER test yielded a good statistical credibility in the ER tests with COV values averaging 2.50%
- Of the HMA fracture parameters evaluated, tensile strain (ϵ_t) was not very effective to statistically differentiate the crack resistance potential of mixes based on the ANOVA and Tukey's HSD statistical analysis.
- Of the HMA fracture parameters evaluated, the tensile modulus (E_t) and *FE Index* exhibited more data variability, with the highest COV values averaging 20.0% and 18.0%, respectively – however, all are still acceptably within the 30% COV threshold.
- The elastic recovery (ductility) exhibited good statistical correlation to *stiffness* from the BBR performed at -12°C and to the *m-value* performed at -18°C , with R^2 exceeding 60%, respectively.
- The asphalt-binder low temperature properties exhibited good statistical correlation with the tensile strain (ϵ_t) and *FE Index* from the M-OT test – suggesting that the asphalt-binder *stiffness*, *ER*, and *m-value* can be used as good predictors of these HMA fracture properties, with a predictive certainty/accuracy exceeding 60%.
- No clear trend was found between the evaluated asphalt-binder low temperature properties with the following HMA fracture properties: peak load (P), tensile strength (σ_t), and fracture energy (FE) obtained from the M-OT test. This finding might suggest a shortcoming in the ability of the asphalt-binder low temperature properties obtained from the BBR and ER tests to predict these HMA fracture parameters. Or may simply be related to the specific asphalt-binders, HMA mixes, and/or test conditions considered in this study.
- The asphalt-binder low-temperature properties obtained from the BBR and ER, namely the *stiffness*, *m-value*, and *ER*, indicated statistical reliability with lower than 50% certainty/accuracy as predictors of the field cracking (reflective) performance of the HMA mixes.
- For modeling reflective cracking initiation, i.e., to time instance when cracking starts to appear on the overlaid surface, whilst accounting for traffic loading in terms of ESALs, the fracture energy (FE), peak load (P), and tensile strength (σ_t) exhibited the most promising potential to correlate and predict field reflective cracking performance of HMA mixes. However, once cracking has started (i.e., crack

propagation), *FE* and *FE Index* exhibited superiority in statistically correlating with the field performance – the R^2 values were over 60%.

- For modeling the entire reflecting cracking response-curve (i.e., both crack initiation and propagation), the tensile modulus (E_t), peak load (P) and tensile strength (σ_t) exhibited superiority correlations over the other HMA fracture parameters, with R^2 values exceeding 60%.
- Of all the HMA fracture parameters evaluated, the *FE* and *FE Index* exhibited the highest statistical correlation with the field performance data – with R^2 values as high as 90% and 94%, respectively.

In general, while the asphalt-binder low temperature properties (*ER*, *m-value*, and *S*) exhibited promising potential to predict the HMA fracture properties from the M-OT test, namely *tensile strain* (ϵ_t) and *Fracture Energy Index (FE Index)*, with a coefficient of determination (R^2) greater than 60%, this was not the case with the field cracking performance data. Good statistical correlations and a prediction certainty/accuracy of over 60% (i.e., $R^2 > 60\%$) were obtained only for the case where the field cracking performance data was analyzed and normalized to an equivalent number of traffic loading ESALs. This means that for asphalt-binder-field correlations, the field cracking performance (i.e., %cracking) must preferably be analyzed as a function of traffic loading (i.e., normalized to the same MESALs) in order to achieve better correlations and high predictive certainty/accuracy with the asphalt-binder low temperature properties. However, these findings may also suggest that the asphalt-binder low temperature properties from the ER and BBR tests must be interpreted and applied cautiously when directly relating to and/or predicting the field cracking performance of the corresponding HMA mixes.

The monotonic-loading OT test has exhibited promising potential as a repeatable test (COV < 30%) for evaluating and quantifying the cracking resistance potential of HMA mixes in the laboratory relative to field performance of in-service highway sections. In particular, the HMA fracture parameters *FE*, tensile strength (σ_t), *FE Index*, and peak load (P_{max}) from the monotonic-loading OT test were satisfactorily able to differentiate the HMA mixes (statistical grouping ≥ 2) and also correlated well ($R^2 > 60\%$) with the measured field cracking performance data.

Preliminary pass-fail screening thresholds were also tentatively proposed in the document – however, more studies are strongly warranted including continued field performance monitoring of the six in-service highway sections evaluated in this study to build up on the findings reported herein and refine/consolidate the screening criteria proposed in this study. The primary goal of this study was to correlate and preliminarily validate the laboratory asphalt binder low temperature properties and monotonic-loading OT test to field crack performance of in-service highway sections, the proposed correlations require a greater amount of data (field and laboratory) to be stronger and can be used directly to predict cracking and fracture behavior of HMA.

Nonetheless, these findings pertain only to the asphalt-binders, HMA mixes, and highway sections evaluated in this study. Therefore, the overall findings may not be exhaustive. However, the inclusion of more asphalt-binders, HMA mixes, and field highway sections

(both cracked and un-cracked) from the Texas DSS is recommended in future studies to further supplement the findings reported in this paper.

7.3. Significance and Application of the Study Results and Findings

From an academic and practical perspective, this study represents an important contribution to the asphalt mixes evaluation in the laboratory taking into account that many of the parameters obtained from commonly laboratory tests still require validation with field performance, suggesting a shortcoming in the ability of this parameters to evaluate/characterize HMA mixes.

This study preliminarily validates and correlate some asphalt binder/HMA fracture properties to field performance data, assess the ability of this parameters to statistically differentiate between mixes taking into account their statistical variance. Suggesting the most promising parameters for HMA/asphalt binder reflective cracking evaluation.

This study suggest that the asphalt-binder low temperature properties from the ER and BBR tests must be interpreted and applied cautiously when directly relating to and/or predicting the field cracking performance of the corresponding HMA mixes, by contrast, proposed HMA fracture parameters *FE*, tensile strength (σ_t), *FE Index*, and peak load (P_{max}) from the monotonic-loading OT test as a good predictors of field cracking performance.

7.4. Limitations and Challenges of the Study

The main limitations of the study are summarized as follows:

- Although the influence of temperature on the reflective cracking phenomenon has been reported in the literature, this effect was not considered thoroughly in the study, this effect should be included within the study matrix and assess the ability to prediction of the evaluated HMA/Asphalt Binder parameters.
- For the Bending Beam Rheometer and Elastic Recovery Test, only two and one temperature were evaluated respectively, given the viscoelastic-thermoplastic behavior of asphalt binders, other test temperatures must be evaluated in order to compare the results.
- Only six highways test sections, with four HMA mix design characteristics were evaluated, the field data availability continuous been a challenge or otherwise, because of the needs of costly long-term performance monitoring. Thus, having a long-term database (although costly) is vital to help with correlating and validating some of these laboratory tests with field cracking performance data.
- The analysis is carried out on highways test sections built with defined mix designs characteristics, it was not possible to evaluate the isolated effect of asphalt on the field performance of mixes, setting/fixing the other design characteristics (i.e. aggregates, asphalt content, etc.)

Lastly, it should be noted that the results presented herein pertain to the laboratory test conditions, HMA mixes, and highway sections evaluated in this study – therefore, the overall findings and conclusions may not be exhaustive.

7.5. Recommendations for Future Research

Future research studies should focus on constructing new pass-fail screening criteria for the HMA fracture parameters FE , tensile strength (σ_t), $FE Index$, and peak load (P_{max}) from the monotonic-loading OT test, these studies should include more HMA mixes and field highway sections (both cracked and un-cracked). If more test sections are included acceptability thresholds curves for each parameters could be constructed.

On the other hand, the researchers should study other laboratory test proposed in the literature related to asphalt binder/HMA cracking evaluation in order to further analyze the available laboratory tests.

REFERENCES

- [1] Z. G. Ghauch and G. G. Abou-Jaoude, "Strain response of hot-mix asphalt overlays in jointed plain concrete pavements due to reflective cracking," *Comput. Struct.*, vol. 124, pp. 38–46, 2013.
- [2] L. G. Loria-Salazar, "Reflective Cracking of Flexible Pavements : Literature Review , Analysis Models , and Testing Methods," *Analysis*, 2008.
- [3] E. R. Brown, P. S. Kandhal, and J. Zhang, "Performance testing for hot mix asphalt," *NCAT Rep. 01-05*, no. November, p. 72, 2001.
- [4] J. W. Button *et al.*, "Transportation Research Circular E-C068: New Simple Performance Tests for Asphalt Mixes.," *Transp. Res. Board Natl. Acad.*, no. September, 2004.
- [5] N. Dhakal, M. A. Elseifi, and Z. Zhang, "Mitigation strategies for reflection cracking in rehabilitated pavements – A synthesis," *Int. J. Pavement Res. Technol.*, vol. 9, no. 3, pp. 228–239, 2016.
- [6] S. Hu, F. Zhou, and T. Scullion, "Reflection Cracking-Based Asphalt Overlay Thickness Design and Analysis Tool," *Transp. Res. Rec. J. Transp. Res. Board*, vol. 2155, pp. 12–23, 2010.
- [7] X. Qiu, J. Ling, and F. Wang, "Concrete pavement rehabilitation procedure using resonant rubblization technology and mechanical–empirical based overlay design," *Can. J. Civ. Eng.*, vol. 41, no. 1, pp. 32–39, 2013.
- [8] G. S. Cleveland, J. W. Button, and R. L. Lytton, "Geosynthetics in Flexible and Rigid Pavement," *Fhwa/Tx-02/1777- 1*, vol. 7, no. 2, 2002.
- [9] F. Zhou *et al.*, "Field Validation of Laboratory Tests to Assess Cracking Resistance of Asphalt Mixtures: An Experimental Design," 2016.
- [10] S. I. Lee, A. N. M. Faruk, X. Hu, B. Haggerty, and L. F. Walubita, "ALTERNATIVE LABORATORY TEST METHOD AND CORRELATIONS TO 2 ESTIMATE MODULUS OF RUPTURE OF CEMENT-TREATED BASE MATERIALS," *Transp. Res. Rec. J. Transp. Res. Board*, p. 561869, 2016.
- [11] B. Sheng and W. V. Ping, "Evaluation of Florida Asphalt Mixes for Crack Resistance Properties using the Laboratory Overlay Test Procedure," *Florida DoT*, no. January, p. 176, 2016.
- [12] L. F. Walubita, A. N. M. Faruk, A. E. Alvarez, R. Izzo, B. Haggerty, and T. Scullion, "Laboratory Hot-Mix Asphalt Cracking Testing," *Transp. Res. Rec. J. Transp. Res. Board*, vol. 2373, no. 1, pp. 81–88, 2013.
- [13] F. Zhou and T. Scullion, "Upgraded Overlay Tester and Its Application To Characterize Reflection Cracking Resistance of Asphalt Mixtures," vol. 7, no. 2, 2003.
- [14] R. L. Lytton, "Use of geotextiles for reinforcement and strain relief in asphalt

- concrete,” *Geotext. Geomembranes*, vol. 8, no. 3, pp. 217–237, 1989.
- [15] L. F. Walubita, A. N. M. Faruk, J. Zhang, and X. Hu, “Characterizing the cracking and fracture properties of geosynthetic interlayer reinforced HMA samples using the Overlay Tester (OT),” *Constr. Build. Mater.*, vol. 93, pp. 695–702, 2015.
- [16] D. Chen, Q. Huang, and J. Ling, “Shanghai ’ s Experience on Utilizing the Rubblization,” *J. Perform. Constr. Facil.*, vol. 22, no. December, pp. 398–407, 2008.
- [17] X. Hu and L. F. Walubita, “Influence of asphalt-binder source on CAM mix rutting and cracking performance: A laboratory case study,” *Int. J. Pavement Res. Technol.*, vol. 8, no. 6, pp. 419–425, 2015.
- [18] T. W. Kennedy *et al.*, *Superior Performing Asphalt Pavements (Superpave): The Product of the SHRP Asphalt Research Program*. Washington, DC: Strategic Highway Research Program, 1994.
- [19] AASHTO T313-05, “Standard Method of Test for Determining the Flexural Creep Stiffness of Asphalt Binder Using the Bending Beam Rheometer (BBR),” *Stand. Specif. Transp. Mater. Methods Sampl. Test.*, 2005.
- [20] ASTM D-6648, “Standard Test Method for Determining the Flexural Creep Stiffness of Asphalt Binder Using the Bending Beam Rheometer (BBR),” *Am. Soc. Test. Mater.*, vol. i, no. Reapproved 2016, pp. 1–15, 2019.
- [21] ASTM D-6084, “Standard Test Method for Elastic Recovery of Asphalt Materials by Ductilometer,” *Am. Soc. Test. Mater.*, vol. i, pp. 1–5, 2019.
- [22] E. Y. Hajj, L. G. L. Salazar, and P. E. Sebaaly, “Methodologies for Estimating Effective Performance Grade of Asphalt Binders in Mixtures with High Recycled Asphalt Pavement Content,” *Transp. Res. Rec. J. Transp. Res. Board*, vol. 2294, no. 1, pp. 53–63, 2013.
- [23] K. A. Ghuzlan and G. G. Al-Khateeb, “Selection and verification of performance grading for asphalt binders produced in Jordan,” *Int. J. Pavement Eng.*, vol. 14, no. 2, pp. 116–124, 2013.
- [24] C. Nicholls, “BitVal - Analysis of Available Data for Validation of Bitumen Tests,” *Rep. Phase 1 BitVal Proj.*, 2005.
- [25] H. A. Tabatabaee and H. Bahia, “Field Validation of a Thermal Cracking Resistance Specification Framework for Modified Asphalt,” *Transp. Res. Rec. J. Transp. Res. Board*, vol. 2505, no. 60, pp. 41–47, 2015.
- [26] A. Diab, M. Enieb, and D. Singh, “Influence of aging on properties of polymer-modified asphalt,” vol. 196, pp. 54–65, 2019.
- [27] D. Lo Presti, “Recycled Tyre Rubber Modified Bitumens for road asphalt mixtures : A literature review q,” vol. 49, pp. 863–881, 2013.
- [28] J. Gong *et al.*, “Performance evaluation of warm mix asphalt additive modified epoxy asphalt rubbers,” *Constr. Build. Mater.*, vol. 204, pp. 288–295, 2019.

- [29] C. Chen, J. H. Podolsky, R. C. Williams, and E. W. Cochran, "Laboratory investigation of using acrylated epoxidized soybean oil (AESO) for asphalt modification," *Constr. Build. Mater.*, vol. 187, pp. 267–279, 2018.
- [30] L. F. Walubita, A. N. M. Faruk, A. E. Alvarez, and T. Scullion, "The Overlay Tester (OT): Using the Fracture Energy Index concept to analyze the OT monotonic loading test data," *Constr. Build. Mater.*, vol. 40, pp. 802–811, 2013.
- [31] N. Lee and S. A. M. Hesp, "Low temperature fracture toughness of polyethylene-modified asphalt binders," *Transp. Res. Rec.*, vol. 1436, pp. 54–59, 1994.
- [32] J. D'Angelo, G. Reinke, H. Bahia, H. Wen, C. M. Johnson, and M. Marasteanu, "Development in Asphalt Binder Specifications (E-C147)," *Transp. Res. BOARD*, no. December, 2010.
- [33] L. F. Walubita, A. N. M. Faruk, X. Hu, R. Malunga, E. Z. Teshale, and T. Scullion, "The Search for a Practical Laboratory Cracking Test for Evaluating Bituminous (HMA) Mixes," pp. 178–185, 2014.
- [34] X. Li, N. Gibson, and J. Youtcheff, "Evaluation of asphalt mixture cracking performance using the monotonic direct tension test in the AMPT," *Road Mater. Pavement Des.*, vol. 18, no. 0, pp. 447–466, 2017.
- [35] L. F. Walubita, A. N. Faruk, Y. Koochi, R. Luo, and T. Scullion, "The Overlay Tester (OT): Comparison with Other Crack Test Methods and Recommendations for Surrogate Crack Tests," vol. 7, no. 2, p. 180, 2013.
- [36] F. Zhou and T. Scullion, "Overlay tester: a rapid performance related crack resistance test," vol. 7, no. 2, p. FHWA/TX-04/0-4467-2, 2005.
- [37] B. P. Jamison, "Laboratory Evaluation of Hot-Mix Asphalt Concrete Fatigue Cracking Resistance," no. December, 2010.
- [38] B. Huang, X. Shu, and Y. Tang, "COMPARISON OF SEMI-CIRCULAR BENDING AND INDIRECT TENSILE STRENGTH TESTS FOR HMA MIXTURES," *Adv. Pavement Eng. Adv. ASCE*, no. ASCE, pp. 1–12, 2005.
- [39] F.-L. Tsai, R. L. Lytton, and S. Lee, "Prediction of Reflection Cracking in Hot-Mix Asphalt Overlays," *Transp. Res. Rec. J. Transp. Res. Board*, vol. 2155, no. 1, pp. 43–54, 2010.
- [40] M. A. Elseifi and I. L. Al-Qadi, "A Simplified Overlay Design Model against Reflective Cracking Utilizing Service Life Prediction," *Road Mater. Pavement Des.*, vol. 5, no. 2, pp. 169–191, 2004.
- [41] B. W. Tsai and C. L. Monismith, "Influence of asphalt binder properties on the fatigue performance of asphalt concrete pavements," *2005 J. Assoc. Asph. Paving Technol. From Proc. Tech. Sess. Vol 74*, vol. 74, no. March, pp. 733–789, 2005.
- [42] K. D. Stuart and W. S. Mogawer, "Validation of the Superpave Asphalt Binder Fatigue Cracking Parameter Using the FHWA's Accelerated Loading Facility," *Fed. Highw.*

Adm., 2003.

- [43] J. Zhang, A. N. M. Faruk, P. Karki, I. Holleran, X. Hu, and L. F. Walubita, "Relating asphalt binder elastic recovery properties to HMA cracking and fracture properties," *Constr. Build. Mater.*, vol. 121, pp. 236–245, 2016.
- [44] H. U. . Bahia, D. I. Hanson, M. Zeng, H. . Zhai, M. A. . Khatri, and R. M. Anderson, "NCHRP Report 459. Characterization of Modified Asphalt Binders in Superpave Mix Design," 2001.
- [45] D. Anderson, Y. Hir, M. Marasteanu, J.-P. Planche, D. Martin, and G. Gauthier, "Evaluation of Fatigue Criteria for Asphalt Binders," *Transp. Res. Rec. J. Transp. Res. Board*, vol. 1766, no. January, pp. 48–56, 2001.
- [46] M. W. Witczak, K. Kaloush, T. Pellinen, M. El-Basyouny, and H. Von Quintus, *Simple Performance Test for Superpave Mix Design. NCHRP, Report 465.*, vol. 1540, no. 9. 2002.
- [47] ASTM D-6373, "Standard Specification for Performance Graded Asphalt Binder," *Am. Soc. Test. Mater.*, 2016.
- [48] AASHTO M320, "Standard Specification for Performance-Graded Asphalt Binder," *Am. Assoc. State Highw. Transp. Off.*, 2015.
- [49] S. A. M. Hesp *et al.*, "Asphalt pavement cracking: Analysis of extraordinary life cycle variability in eastern and northeastern Ontario," *Int. J. Pavement Eng.*, vol. 10, no. 3, pp. 209–227, 2009.
- [50] S. Tabib, O. Khuskivadze, P. Marks, E. Nicol, H. Ding, and S. A. M. Hesp, "Pavement performance compared with asphalt properties for five contracts in Ontario," *Constr. Build. Mater.*, vol. 171, pp. 719–725, 2018.
- [51] C. S. Clopotel and H. U. Bahia, "Importance of elastic recovery in the DSR for binders and mastics," *Eng. J.*, vol. 16, no. 4, pp. 99–106, 2012.
- [52] ASTM D-7405, "Standard Test Method for Multiple Stress Creep and Recovery (MSCR) of Asphalt Binder Using a Dynamic Shear Rheometer," *Am. Soc. Test. Mater.*, vol. i, pp. 13–16, 2019.
- [53] J. Zhu, B. Birgisson, and N. Kringos, "Polymer modification of bitumen: Advances and challenges," *Eur. Polym. J.*, vol. 54, no. 1, pp. 18–38, 2014.
- [54] W. Jensen and M. Abdelrahman, "Crumb Rubber in Performance-Graded Asphalt Binder," vol. 01, no. November, p. 160, 2006.
- [55] F. Bonemazzi, V. Braga, R. Corrieri, C. Giavarini, and F. Sartori, "Characteristics of Polymers and Polymer-Modified Binders," *Transp. Res. Rec. J. Transp. Res. Board*, vol. 1535, pp. 36–47, 2007.
- [56] M. da C. C. Lucena, S. de A. Soares, and J. B. Soares, "Characterization and thermal behavior of polymer-modified asphalt," *Mater. Res.*, vol. 7, no. 4, pp. 529–534, 2006.

- [57] W. Mogawer, A. Austerman, M. E. Kutay, and F. Zhou, "Evaluation of Binder Elastic Recovery on HMA Fatigue Cracking using Continuum Damage and Overlay Test Based Analyses," *Road Mater. Pavement Des.*, vol. 12, no. 2, pp. 345–376, 2011.
- [58] A. Golalipour, "Modification of Multiple Stress Creep and Recovery Test Procedure and Usage in Specification," *Master Thesis*, 2011.
- [59] G. Nsengiyumva, "Development of Semi-Circular Bending (SCB) Fracture Test for Bituminous Mixtures," 2015.
- [60] T. Bennert, E. Haas, and E. Wass, "Indirect Tensile Test (IDT) to Determine Asphalt Mixture Performance Indicators during Quality Control Testing in New Jersey," *Transp. Res. Rec. J. Transp. Res. Board*, p. 036119811879327, 2018.
- [61] L. F. Walubita, S. I. Lee, A. N. Faruk, T. Scullion, S. Nazarian, and I. Abdallah, "Texas Flexible Pavements and Overlays : Year 5 Report — Complete Data Documentation Technical Report 0-6658-3," 2017.
- [62] L. F. Walubita *et al.*, "Texas Flexible Pavements and Overlays: Year 1 Report - Test Sections, Data Collection, Analyses, and Data Storage System," vol. 7, no. 2, 2012.
- [63] TxDOT, "Test procedure for Overlay Test," 2017.
- [64] J. Zhang, G. S. Simate, S. Ick, S. Hu, and L. F. Walubita, "Relating asphalt binder elastic recovery properties to HMA crack modeling and fatigue life prediction," *Constr. Build. Mater.*, vol. 111, pp. 644–651, 2016.
- [65] J. A. Daecon, J. T. Harvey, A. Tayebali, and C. L. Monismith, "Influence of Binder Loss Modulus on the Fatigue Performance," 1997.
- [66] S. I. Lee, A. N. M. Faruk, and L. F. Walubita, "Comparison of Fracture Cracking Parameters from Monotonic Loading Tests," *Transp. Res. Rec. J. Transp. Res. Board*, vol. 2576, no. 2576, pp. 19–27, 2016.
- [67] L. F. Walubita, A. N. Faruk, G. Das, H. A. Tanvir, J. Zhang, and T. Scullion, "The Overlay Tester: A Sensitivity Study to Improve Repeatability and Minimize Variability in the Test Results," vol. 7, no. 2, 2012.
- [68] E. Date and O. Tester, "Test Procedure for OVERLAY TEST TxDOT Designation : Tex-248-F," pp. 2–7, 2009.
- [69] Y. R. Kim and H. Wen, "Fracture energy from indirect tension testing," *Asph. Paving Technol. 2002, March 18, 2002 - March 20, 2002*, vol. 71, no. August, pp. 779–793, 2002.
- [70] TxDOT, "Indirect Tensile Strength Test," *TxDOT Des. Tex-226-F*, no. 200, pp. 2–4, 2014.
- [71] L. F. Walubita, G. S. Simate, and J. ho Oh, "Characterising the ductility and fatigue crack resistance potential of asphalt mixes based on the laboratory," no. October 2010, 2015.

- [72] L. F. Walubita, G. S. Simate, E. Ofori-abebrasse, A. Epps, R. L. Lytton, and L. E. Sanabria, "Mathematical formulation of HMA crack initiation and crack propagation models based on continuum fracture-mechanics and work-potential theory," *Int. J. Fatigue*, vol. 40, pp. 112–119, 2012.
- [73] C. E. Brown, "Multivariate Analysis of Variance," in *Applied Multivariate Statistics in Geohydrology and Related Sciences*, 1998.
- [74] S. M. Ross, *Introduction to Probability and Statistics for Engineers and*, 4th ed., vol. 53, no. 9. UC – Berkeley, USA: Elsevier, Academic Press (AP), 2009.
- [75] L. F. Walubita *et al.*, "Use of grid reinforcement in HMA overlays – A Texas field case study of highway US 59 in Atlanta District," *Constr. Build. Mater.*, 2019.
- [76] M. Oshone, E. V. Dave, and J. E. Sias, "Asphalt mix fracture energy based reflective cracking performance criteria for overlay mix selection and design for pavements in cold climates," *Constr. Build. Mater.*, vol. 211, pp. 1025–1033, 2019.

APPENDICES

A. Database

The information obtained from the DSS used throughout this investigation for data analysis are included in the appendix folder as follows:

- The *Bending Beam Rheometer* test results is included in the Appendix folder, see the file 'BBRTTestResults.txt'.
- The *Elastic Recovery* test results is included in the Appendix folder, see the file 'ERTTestResults.txt'.
- The *Monotonic Loading overlay* test results is included in the Appendix folder, see the file 'MOTTTestResults.txt'.
- The Field Performance measurements is included in the Appendix folder, see the file 'FieldMeasurements.txt'.

B. R Codes Results

The script files used throughout this investigation for data analysis are included in the appendix folder as follows:

- Peak Load: ANOVA and Tukey's HSD analysis: ANOVA and Tukey's HSD folder – file 'Tukey Peak Load.pdf'.
- Tensile Strength: ANOVA and Tukey's HSD analysis: ANOVA and Tukey's HSD folder – file 'Tensile Strength Tukey.pdf'.
- Tensile Strain: ANOVA and Tukey's HSD analysis: ANOVA and Tukey's HSD folder – file 'Tensile Strain Tukey.pdf'.
- Tensile Modulus: ANOVA and Tukey's HSD analysis: ANOVA and Tukey's HSD folder – file 'TM Tukey.pdf'.
- Fracture Energy: ANOVA and Tukey's HSD analysis: ANOVA and Tukey's HSD folder – file 'FE Tukey.pdf'.
- Fracture Energy Index: ANOVA and Tukey's HSD analysis: ANOVA and Tukey's HSD folder – file 'FEI Tukey.pdf'.